Pollen tube-triggered accumulation of NORTIA at the filiform apparatus facilitates fertilization in *Arabidopsis thaliana*

Jing Yuan[1,2*], Yan Ju[1,2*], Daniel S. Jones[4,5], Weiwei Zhang[2,3], Noel Lucca[1,2], Christopher J. Staiger[1,2,3], and Sharon A. Kessler[1,2,**]

[1]Department of Botany and Plant Pathology, Purdue University, West Lafayette, Indiana USA
[2]Purdue Center for Plant Biology, Purdue University, West Lafayette, Indiana USA
[3]Department of Biological Sciences, Purdue University, West Lafayette, Indiana USA
[4]Biology Department, The University of North Carolina at Chapel Hill, Chapel Hill, North Carolina USA (current address)
[5]Department of Microbiology and Plant Biology, University of Oklahoma, Norman, Oklahoma USA
*These authors contributed equally

** Corresponding author
Email: sakessler@purdue.edu

Abstract

During gamete delivery in *Arabidopsis thaliana*, intercellular communication between the attracted pollen tube and the receptive synergid cell leads to subcellular events in both cells culminating in the rupture of the tip-growing pollen tube and release of the sperm cells to achieve double fertilization. Live imaging of pollen tube reception revealed dynamic subcellular changes that occur in the female synergid cells. Pollen tube arrival triggers the trafficking of NORTIA (NTA) MLO protein from Golgi-associated compartments and the accumulation of endosomes at or near the synergid filiform apparatus, a membrane-rich region that acts as the site of communication between the pollen tube and synergids. Domain swaps and site-directed mutagenesis reveal that NTA's C-terminal cytoplasmic tail with its calmodulin-binding domain influences the subcellular localization and function of NTA in pollen tube reception and that early

accumulation of NTA at the filiform apparatus is sufficient for MLO function in pollen tube reception.

Key words

MLO, Pollination, gametophyte, synergid, pollen tube reception, calmodulin binding domain

Introduction

Intercellular communication is central to the proper development and maintenance of all multicellular organisms. During this communication, signals from one cell are perceived by receptors in another cell and translated into various subcellular responses. These responses include signal transduction cascades leading to transcription of other genes, calcium signaling, and trafficking of proteins to different organelles or regions of the cell. A well-studied example of signal-induced protein trafficking in plant development is the redistribution of the PIN polar auxin transporters to different sides of the cell during important developmental events such as embryo patterning, leaf initiation and lateral root initiation (Petrasek et al., 2006; Naramoto, 2017; Salanenka et al., 2018). In plants, most intercellular communication occurs between cells that are genetically identical and connected by adjoining cell walls. One exception is pollination, in which pollen (the male gametophyte) is released from an anther, transported to a receptive stigma, and produces a tip-growing pollen tube that grows through the female tissues of the pistil and delivers the two sperm cells to the female gametophyte (also known as the embryo sac, Figure 1A). The pollen tube's journey through the pistil requires cell-to-cell interactions with the female that allows water and nutrient uptake and enables the detection of cues important for guidance toward the female gametes (Johnson et al., 2019).

In the model plant *Arabidopsis thaliana*, complex signaling events ranging from pollen landing on the stigma to fusion of gametes occur over several hours. Most of our knowledge about the signaling pathways involved along the pollen tube's journey through the female is limited to the

final stages of pollination and involve a highly specialized pair of female gametophyte cells known as synergids. During female gametophyte development, meiosis followed by three rounds of mitosis produce the egg cell and central cell along with 2 synergid cells flanking the egg cell and 3 antipodal cells on the chalazal end of the embryo sac (Drews and Yadegari, 2002), Figure 1A). The synergid cells are accessory cells that control the behavior of the pollen tube during the final stages of pollination. Before pollen tube arrival, they secrete cysteine-rich LURE peptides that act as short-range pollen tube attractants that are recognized by receptor-like kinases in the tip of the pollen tube to regulate the direction of pollen tube growth and guide the pollen tube to the micropyle of the ovule (Okuda et al., 2009; Takeuchi and Higashiyama, 2016; Wang et al., 2016). After pollen tube arrival, the synergids communicate with the pollen tube to induce changes that result in pollen tube rupture and delivery of the sperm cells (Kessler and Grossniklaus, 2011; Johnson et al., 2019). Thus, synergids are critical for ensuring that double fertilization can occur to produce seeds.

In Arabidopsis, live imaging has been used to examine the behavior of both the pollen tube and the synergids during the process of pollen tube reception. A pollen tube follows the gradient of LURE attractants, enters the micropyle of the ovule, and pauses its growth for 30 min to 1 h just outside the receptive synergid (Iwano et al., 2012; Denninger et al., 2014; Ngo et al., 2014). During this pause in pollen tube growth, communication occurs between the pollen tube and the synergids leading to subcellular changes and ultimately the death of both the pollen tube and the receptive synergid. Cytoplasmic calcium oscillations occur in both the tip of the pollen tube and in the 2 synergid cells during this communication phase. Cytoplasmic calcium levels continue to increase in both cell types until the pollen tube starts to grow again and bursts to release the sperm cells, a catastrophic event for both the pollen tube and the receptive synergid, which also degenerates (Iwano et al., 2012; Denninger et al., 2014; Ngo et al., 2014). Mutations in genes that regulate communication between the synergids and pollen tube during

pollen tube reception result in a pollen tube overgrowth phenotype in which the pollen tubes are attracted normally to the ovules, but do not get the signal to burst and release the sperm cells. Presumably, synergid-induced changes in the cell wall of the pollen tube tip do not occur in these mutants, therefore the pollen tube continues to grow and coil inside the embryo sac. Synergid-expressed genes that participate in pollen tube reception include the FERONIA (FER) receptor-like kinase, the GPI-anchored protein LORELEI (LRE), and the Mildew Resistance Locus-O (MLO) protein NORTIA (NTA, also known as AtMLO7) (Escobar-Restrepo et al., 2007; Capron et al., 2008; Kessler et al., 2010; Ngo et al., 2014; Li et al., 2015; Liu et al., 2016). Mutations in all of these genes lead to the pollen tube overgrowth phenotype due to disruption of the pollen tube-synergid communication pathway.

FER and LRE are necessary for the calcium oscillations that occur in synergids in response to pollen tube arrival (Ngo et al., 2014). In contrast, *nta-1* mutants have $[Ca^{2+}]_{cyto}$ oscillations at lower amplitudes, indicating that NTA may participate in modulating Ca^{2+} fluxes in the synergids during communication with the pollen tube and likely acts downstream of FER and LRE (Ngo et al., 2014). Like all members of the MLO gene family, NTA has seven membrane-spanning domains and a predicted calmodulin-binding domain (CaMBD) in its C-terminal intracellular tail (Devoto et al., 2003; Kusch et al., 2016). Calmodulin (CaM) is a small protein that binds Ca^{2+} and is involved in signal transduction for many cellular processes (Yang and Poovaiah, 2003). We previously showed that the C-terminal domain of NTA could confer pollen tube reception function to the related MLO8 protein (Jones et al., 2017), but the significance of the CaMBD in pollen tube reception remains an open question.

The subcellular localization of these important pollen tube reception proteins is not always predictive of their function in communicating with the pollen tube. As expected for early response proteins, both FER and LRE are expressed in synergid cells where they localize in or

near a specialized region called the filiform apparatus, a membrane rich area located at the micropyle end of the synergids (Huck et al., 2003; Rotman et al., 2003; Escobar-Restrepo et al., 2007; Capron et al., 2008; Li et al., 2015; Lindner et al., 2015; Liu et al., 2016). The filiform apparatus is thought to be important for the secretion of attractant peptides and is the first site of interaction between the pollen tube and synergid cell prior to pollen tube reception (Mansfield et al., 1991; Huang and Russell, 1992; Leshem et al., 2013). In contrast, before pollen tube arrival, NTA is localized to a Golgi-associated compartment within the synergid cell and absent from the filiform apparatus (Jones et al., 2017). At the end of pollen tube reception, NTA protein is only detected at the filiform apparatus, indicating that this protein changes its subcellular localization during pollen tube reception (Kessler et al., 2010). This suggests that pollen tube-triggered regulation of the synergid secretory system may be a crucial subcellular response to pollen tube arrival and that NTA function may be related to its subcellular distribution; however, the precise timing and significance of NTA's redistribution remain unclear.

Here, we use a live-imaging system to further characterize synergid cellular dynamics during pollen tube reception and to determine the timing and significance of the polar redistribution of NTA to the filiform apparatus. To investigate the link between Ca^{2+} and MLO function in pollen tube reception, we assayed the influence of the CaMBD on NTA's function and subcellular distribution through C-terminal truncations and a point mutation disrupting the CaMBD. We show that the polar redistribution of NTA is triggered by the approach of a pollen tube, is important for pollen tube reception, and is facilitated by the CaMBD. While most subcellular compartments remain distributed throughout the synergid cells during pollen tube reception, recycling endosomes respond to pollen tube arrival by accumulating towards the filiform apparatus. Moreover, we show that targeting NTA to the filiform apparatus before pollen tube attraction does not induce synergid cell death.

Results

NORTIA Dynamically Redistributes to the Filiform Apparatus during Pollen Tube Reception

Pollen tube reception requires synergid cells to recognize the approaching pollen tube and to send signals back to the pollen tube that result in release of the sperm cells at the correct time and place so that double fertilization can be completed. Based on static images, we previously reported that NTA-GFP fusion protein localizes to a Golgi-associated compartment in synergids prior to pollen tube attraction (Jones et al., 2017). When imaged after pollen tube reception, NTA-GFP is concentrated at the micropylar end of the synergid (in or near the filiform apparatus) (Kessler et al., 2010). NTA-GFP does not accumulate at the filiform apparatus in *fer* ovules with pollen tube overgrowth, suggesting that FER-mediated signaling during pollen tube reception triggers NTA-GFP redistribution that in turn contributes to the interaction of the synergid with the pollen tube (Kessler et al., 2010). An alternative hypothesis is that pollen tube rupture triggers NTA-GFP redistribution and is a symptom of pollen tube reception rather than an important contributor to the signaling pathway. To distinguish between these two possibilities, we used a semi-*in vivo* pollination system combined with time-lapse spinning disk confocal microscopy to determine the timing of NTA-GFP redistribution during the pollen tube reception process. In the semi-*in vivo* system, pollen tubes grow out of a cut style and are attracted to ovules arranged on pollen germination media (Palanivelu and Preuss, 2006). This system has previously been used to quantify and track pollen tube attraction to ovules and to image $[Ca^{2+}]_{cyto}$ reporters during pollen tube reception (Hamamura et al., 2011; Hamamura et al., 2012; Denninger et al., 2014; Hamamura et al., 2014; Ngo et al., 2014).

To follow subcellular changes in NTA-GFP protein localization before, during, and after pollen tube arrival, we used pollen from plants expressing the pollen-specific *AUTOINHIBITED* Ca^{2+}-*ATPase9*$_{pro}$*::DsRed* (*ACA9*$_{pro}$*::DsRed*) reporter and ovules expressing *NTA*$_{pro}$*::NTA-GFP* in the

160 semi-*in vivo* system. Approximately 4 h after pollination, pollen tubes emerged from the style
161 onto the media and were attracted to ovules (Figure 1B). Fluorescence images in both channels
162 were collected every 5 min from when a pollen tube approached an ovule until after the pollen
163 tube ruptured inside the ovule. In ~83% (n=93) of the ovules that attracted a pollen tube and
164 successfully burst to deliver the sperm cells, NTA-GFP accumulated at the filiform apparatus of
165 the synergids (Figures 1C-E). The rest of the ovules (~17%) attracted pollen tubes that stopped
166 growing in the micropyle and did not rupture. In these ovules, NTA-GFP did not accumulate in
167 the filiform apparatus. To exclude the possibility that prolonged imaging causes stress in
168 synergids which leads to filiform apparatus accumulation of NTA-GFP, we analyzed neighboring
169 ovules that did not attract pollen tubes but were imaged together with ovules that attracted
170 pollen tubes. NTA-GFP did not accumulate at the filiform apparatus in these ovules (n=103)
171 (Figure 1F). Likewise, ovules that were incubated on pollen germination media without a
172 pollinated pistil (n=133, Figures 1F and S1) and imaged over the same time frame did not
173 accumulate NTA-GFP in the filiform apparatus. These data indicate that pollen tube arrival is
174 necessary for NTA-GFP accumulation at the filiform apparatus rather than being retained in the
175 Golgi, and that this accumulation is not an artifact of the semi- *in vivo* imaging system. (Figure
176 1F).
177
178 Our semi-*in vivo* system also allowed us to determine the timing of NTA-GFP accumulation at
179 the filiform apparatus in relation to the position of the pollen tube as it approached the
180 synergids. We defined the 0 min timepoint as the time where the pollen tube just reached the
181 micropylar opening of the ovule (Figure 1C, ovules with yellow stars, Movies S1 and S2). In all
182 cases, the shift of NTA-GFP signal from the Golgi to the filiform apparatus also started from this
183 time point. During the following 30–50 min, pollen tubes grew through the micropyle region of
184 ovule and arrived at the filiform apparatus of the receptive synergid cell. During this time, three
185 quarters to half of the NTA-GFP signal moved to the micropylar end of synergid cells, indicating

that the approach of the pollen tube triggers NTA-GFP accumulation at the filiform apparatus. As reported in Ngo et al., 2014 and Denninger et al., 2014, the arriving pollen tubes paused their growth outside the filiform apparatus for 30–50 min, presumably for cell-to-cell communication. During this period, the NTA-GFP signal continued to shift toward the filiform apparatus. At 70–80 min after pollen tube arrival at the micropyle, NTA-GFP signal was only detected in the filiform apparatus and pollen tubes resumed growth and ruptured to release the sperm cells (Figures 1C, D and Movies S1 and S2). Even though only one of the synergids receives the pollen tube, NTA-GFP accumulated at the filiform apparatus in both synergid cells in response to pollen tube arrival, similar to the activation of $[Ca^{2+}]_{cyto}$ oscillations in both synergids during pollen tube reception reported in (Ngo et al., 2014).

Golgi do not concentrate at the filiform apparatus during pollen tube reception

We previously determined that NTA is sequestered in a Golgi-associated compartment in synergid cells that have not attracted a pollen tube (Jones et al., 2017) . Our live-imaging data suggest that NTA-GFP is selectively moved out of the Golgi and transported to the filiform apparatus in response to pollen tube arrival; however, it is possible that the observed NTA-GFP accumulation at the filiform apparatus is a result of massive reorganization of subcellular compartments. To distinguish between these possibilities, we investigated the behavior of Golgi in synergid cells during pollen tube reception. We used the semi-*in vivo* imaging system described above with a synergid-expressed Golgi marker (Man49-mCherry) co-expressed with NTA-GFP (Jones et al., 2018). In all replicates, the Golgi marker was distributed throughout the synergids, excluded from the filiform apparatus, and co-localized with NTA-GFP as reported previously (Figure 2A, n=93). When a pollen tube approached the synergids, NTA-GFP accumulated at the filiform apparatus region of the synergids as observed previously (Figure 1), but the Golgi-mCherry marker remained consistently distributed throughout the synergid cells and did not concentrate near the filiform apparatus (Figure 2B). In order to examine the

behavior of the Golgi during later stages of pollen tube reception, we used the synergid-expressed Golgi marker line (*LRE$_{pro}$::Man49-mCherry*) and pollen that was expressing GFP (*Lat52$_{pro}$::GFP*). In all cases, the Golgi marker remained randomly distributed throughout the synergid cells, even after pollen tube rupture (Figures 2C-D, Movies S3 and S4, n=106). These results indicate that the accumulation of NTA-GFP at the filiform apparatus during pollen tube reception is not linked to mass redistribution of Golgi.

Endosomes accumulate at the filiform apparatus during pollen tube reception

A signal from the arriving pollen tube seems to trigger the movement of NTA-GFP out of the Golgi-associated compartments. It is possible that pollen tube arrival triggers other changes to synergid subcellular organization. We previously reported the localization of synergid-expressed markers for the ER, peroxisome, endosome and the trans-Golgi Network (TGN) in unfertilized ovules *in vivo* using confocal laser scanning microscopy (Jones et al., 2018). Before pollen tube arrival, SP-mCherry-HDEL (an ER-associated marker), mCherry-SKL (a peroxisome-associated marker), and mCherry-RabA1g (a recycling endosome-associated marker) were all distributed evenly throughout synergid cells (Figures S2-S4 and 3A; (Jones et al., 2018). The TGN-associated marker SYP61 exhibited two types of distribution patterns before pollen tube arrival: in type 1 synergids, the marker accumulated near the filiform apparatus, whereas type 2 synergids displayed a punctate distribution pattern throughout the cells (Figure S3; (Jones et al., 2018). During pollen tube reception, no change was seen in the TGN marker distribution in either type of synergids (Figure S3, C-D, Movies S5 and S6). Likewise, the ER and peroxisome markers maintained a diffuse distribution throughout the synergids and did not accumulate at the filiform apparatus (Figures S2 and S4, Movies S7-10). In contrast, we detected a more dynamic behavior of the endosome marker during pollen tube reception. Endosomes are membrane-bound compartments that are involved in the endocytic membrane transport pathway from the plasma membrane to the vacuole. Endosomes also transport molecules from

the Golgi and either continue to the vacuole or recycle back to the Golgi (Stoorvogel et al., 1991). We previously reported that mCherry-RabA1g is distributed throughout synergid cells and had some overlap with NTA-GFP in synergids of unpollinated ovules (Jones et al., 2018). Using the semi-*in vivo* system, we confirmed that before pollen tube arrival, mCherry-RabA1g distributed throughout synergid cells (Figure 3A). Interestingly, as pollen tubes approached, the endosome marker started to accumulate in the filiform apparatus region of the synergid cells (Figures 3A and B). By the time pollen tube reception was completed, most of the endosome signal was concentrated at or near the filiform apparatus (Figures 3B-F and S5, Movies S11 and S12). These results indicate that the RabA1g endosome compartments have a distinct response to pollen tube arrival and may play a role in facilitating the intercellular signaling pathway that occurs between the synergids and the pollen tube.

Pollen tube-independent targeting of NTA to the filiform apparatus is not toxic to the synergids

The selective targeting of NTA-GFP from the Golgi to the filiform apparatus during pollen tube arrival (Figures 1 and 2) suggests that NTA trafficking to the pollen tube/synergid interface is important for the intercellular communication process that occurs between the pollen tube and synergids. In *nta-1* mutants, around 30% of ovules display pollen tube overgrowth and fail to complete double fertilization, but the other 70% are fertilized normally (Kessler et al., 2010). This indicates that NTA is not absolutely required for pollen tube reception, but may function as a modifier of the signaling pathway. Since FER signaling in the synergids leads to cell death as pollen tube reception is completed (Huck et al., 2003; Rotman et al., 2003; Escobar-Restrepo et al., 2007), NTA trafficking to the filiform apparatus could be a mechanism to regulate this death and would thus require sequestration of “toxic” NTA in the Golgi before pollen tube arrival. To test this hypothesis, we took advantage of sequence variation leading to differential subcellular

264 localization of MLO proteins to manipulate the subcellular localization of NTA. When expressed
265 in synergids, other proteins from the Arabidopsis MLO family have different subcellular
266 localization patterns, indicating that specific sequences within the MLOs direct them to different
267 parts of the secretory system (Jones and Kessler, 2017). MLO1-GFP localizes in the filiform
268 apparatus when it is ectopically expressed under control of the synergid-specific *MYB98*
269 promoter and cannot complement the *nta-1* pollen tube reception phenotype (Jones et al., 2017,
270 and Figure 4B). Domain swaps between different regions of NTA and MLO1 revealed that the
271 C-terminal cytoplasmic tail including the CaMBD of MLO1 (NTA-MLO1^{CTerm}, see diagram in
272 Figure 4C) was sufficient to direct the fusion protein to the filiform apparatus region of the
273 synergids, in a pattern very similar to MLO1-GFP (Figure 4B). Quantification of the GFP signal
274 along the length of the synergids from the chalazal end to the filiform apparatus in the NTA-
275 GFP, NTA-MLO1^{Cterm}-GFP, and MLO1-GFP confirmed that the MLO1 tail was sufficient to
276 cause NTA protein to accumulate at the filiform apparatus (Figure 4D). In all MLO1-GFP and
277 NTA-MLO1^{Cterm}-GFP ovules, the majority of GFP signal was detected in the lower 20-40% of the
278 synergids and most of the signal overlapped with the diffuse FM4-64 staining in the filiform
279 apparatus (Figure 4E). In contrast, wild-type NTA-GFP is excluded from the filiform apparatus
280 (Figure 4A and (Jones et al., 2017).
281
282 The successful manipulation of NTA subcellular localization provided a tool for determining the
283 functional relevance of NTA redistribution. We transformed the NTA-MLO1^{CTerm}-GFP construct
284 into *nta-1* plants and used the percentage of unfertilized ovules as a measurement for the ability
285 of the fusion construct to complement the *nta-1* phenotype of unfertilized ovules caused by
286 pollen tube overgrowth (Kessler et al., 2010). Synergid-expression of NTA-MLO1^{CTerm}-GFP
287 rescued the *nta-1* pollen tube reception phenotype (Figure 4F), indicating that 1) the MLO1^{CTerm}
288 domain is functionally equivalent to the NTA^{CTerm} domain when the protein is localized in the

289 filiform apparatus and 2) premature targeting of NTA to the filiform apparatus is not toxic to
290 synergid cells.
291
292 **Disrupting the NTA CaMBD compromises NTA's ability to accumulate at the filiform**
293 **apparatus during pollen tube reception**
294 The dramatic differences in protein localization between NTA-GFP and NTA-MLO1^{CTerm}-GFP
295 revealed that the C-terminal cytoplasmic domain of NTA contains sequences that cause NTA to
296 be sequestered in the Golgi before pollen tube arrival and possibly also to allow for directed
297 transport to the filiform apparatus in response to signals from the arriving pollen tube. The C-
298 terminal cytoplasmic domains of MLO proteins contain a predicted CaMBD followed by an
299 unconserved tail of variable length (Devoto et al., 1999; Kim et al., 2002b; Kim et al., 2002a). A
300 comparison of C-terminal domains (Figure 5A) revealed that NTA and MLO1 share the
301 conserved 20 amino acid 1-8-14 CaM binding motif of hydrophobic residues interspersed with
302 basic residues that define the MLO CaMBD (Kim et al., 2002b), but have different residues
303 surrounding the conserved tryptophan that has been shown to necessary for CaM binding in
304 MLO proteins (Kim et al., 2002b; Kim et al., 2002a). In addition, NTA and MLO1 have different
305 length C-terminal tails after the CaMBD (Figure 5A). In order to determine if the C-terminal tail
306 after the CaMBD is necessary for NTA sequestration in the Golgi before pollen tube arrival, we
307 made a GFP fusion with NTA truncated just after the predicted CaMBD (NTA$^{\Delta 481}$, Figure 5A)
308 expressed under control of the synergid-specific MYB98 promoter. This construct
309 complemented the *nta-1* pollen tube reception phenotype and localized in the Golgi before
310 pollen tube arrival (Figure 5C and 5E), revealing that the C-terminal tail after the CaMBD is not
311 necessary for NTA sequestration or function. We next tested whether disruption of the CaMBD
312 would affect NTA localization and/or function. A point mutation in the conserved tryptophan
313 necessary for CaM-binding in other CaMBDs (Arazi et al., 1995; Yamada et al., 1995; Kim et al.,
314 2002b) was introduced into our NTA-GFP expression construct (NTA^{W458A}, Figure 5A) and

315 transformed into the *nta-1* background. In contrast to wild-type NTA and NTA$^{\Delta 481}$, which result
316 in an even higher fertility in *nta-1* mutants than in the Ws controls, NTA^{W458A} only partially
317 complemented the *nta-1* fertility phenotype (Figure 5E). Before pollen tube arrival, NTA^{W458A} co-
318 localizes with a Golgi marker in synergids similar to wild-type NTA (Figure 5D and Figure S6).
319 However, during pollen tube reception, NTA^{W458A} displays different accumulation patterns that
320 correlate with the ability of the pollen tube to rupture. In our semi-*in vivo* system, ovules with
321 normal pollen tube rupture had at least partial NTA^{W458A} accumulation at the filiform apparatus,
322 while ovules with pollen tube overgrowth did not accumulate NTA^{W458A} at the filiform apparatus
323 (Figure 6). These data reveal that an intact CaMBD enhances NTA's redistribution to the filiform
324 apparatus during pollen tube reception and that NTA accumulation at the filiform apparatus
325 promotes pollen tube rupture, while the C-terminal tail after the CaMBD is dispensable for NTA
326 function.
327
328 The influence of the CaMBD on NTA accumulation at the filiform apparatus could indicate a
329 connection with the calcium oscillations that occur in synergids during signaling with the arriving
330 pollen tube. The receptor-like kinase FER and the GPI-anchored protein LRE are filiform-
331 localized proteins that interact with each other and form a co-receptor for signals from the
332 arriving pollen tube (Escobar-Restrepo et al., 2007; Li et al., 2015; Liu et al., 2016). *fer* and *lre*
333 mutant ovules fail to initiate synergid calcium oscillations at pollen tube arrival and have highly
334 penetrant pollen tube overgrowth phenotypes (Ngo et al., 2014). In *nta-1* mutant ovules,
335 synergids have dampened calcium oscillations and around 30% of ovules carrying the mutation
336 display pollen tube overgrowth (Kessler et al., 2010; Ngo et al., 2014). In both *fer-1* and *lre-7*
337 backgrounds, NTA-GFP does not accumulate at the filiform apparatus in response to signals
338 from the pollen tube (Figure S7 and Kessler, 2010), placing NTA accumulation at the filiform
339 apparatus downstream of both FER and LRE and the calcium oscillations conditioned by these
340 proteins.

Discussion

Synergids respond to a signal from the approaching pollen tube

Successful pollination and production of seeds requires a series of signaling events between the male gametophyte (pollen tube) and both sporophytic and gametophytic cells of the female. In this study, we used live imaging to characterize dynamic subcellular changes that occur in the synergid cells of the female gametophyte in response to the arrival of the pollen tube. We showed that both the NTA protein and endosomes are actively mobilized to the filiform apparatus region where male-female communication occurs during pollen tube reception (Figure 7). Disruption of NTA's CaMBD partially compromised NTA redistribution and function in pollen tube reception, revealing that Ca^{2+} may play a role in the synergid response to the signal from the pollen tube.

The polar accumulation of the RabA1g endosome marker, but not a Golgi marker (Man49-GFP), near the filiform apparatus during pollen tube reception suggests a change in synergid secretory system behavior that is triggered by the approaching pollen tube. Our results with the ER, Golgi, TGN, and peroxisome markers indicate that the mobilization of the RabA1g endosomes toward the approaching pollen tube is not just a symptom of FER signaling triggering synergid cell death that leads to mass disruption of subcellular compartments. Trans-Golgi Network/Early endosomes (TGN/EEs) have been shown to be involved in the trafficking of both secretory and endocytic cargo (Viotti et al., 2010). RabA1g is present in endosomes that are highly sensitive to Brefeldin A in roots, suggesting that they could function as recycling endosomes (Geldner et al., 2009). While the resolution of our live imaging system did not allow us to determine whether NTA completely co-localizes with this compartment, it is tempting to speculate that the RabA1g endosomes are mediating the polar movement of NTA to the filiform apparatus region.

366 Alternatively, these endosomes could be transporting other signaling molecules either to or from
367 the filiform apparatus.
368
369 **Signal-mediated protein trafficking**
370 Signal-mediated regulation of protein trafficking is an elegant mechanism to control the delivery
371 of molecules to the precise location where they are needed for critical signaling events that
372 occur over relatively short time frames. Selective protein targeting similar to NTA movement in
373 response to pollen tube arrival has also been observed during cell-to-cell communication
374 between the egg and sperm cells in Arabidopsis. After pollen tube reception and release of the
375 sperm cells, a signal from the sperm and/or the degenerated synergid cell causes the egg cell to
376 secrete EGG CELL 1 (EC1) peptides that have been stored in punctate compartments in the
377 egg cytoplasm toward the sperm cells. The sperm cells perceive the EC1 signal and, in turn,
378 mobilize the gamete fusogen HAPLESS2/GENERATIVE CELL SPECIFIC1 (HAP2/GCS1) from
379 a cytoplasmic compartment to the cell surface (Sprunck et al., 2012). This controlled movement
380 of proteins that have already been translated and stored facilitates a quick response to activate
381 the egg and sperm for fertilization. Likewise, NTA mobilization to the filiform apparatus region of
382 the synergids as the pollen tube arrives could play a role in sending a signal to the pollen tube
383 that leads to the mobilization of pollen tube proteins that allow the pollen tube to rupture and
384 release the sperm cells. For example, proteins that regulate the integrity of the tip of the pollen
385 tube could be quickly delivered after the “arrival” signal from the synergid is perceived. Recent
386 work on the role of the pollen-expressed ANXUR1 and 2 and BUDDHA PAPER SEAL1 and 2
387 receptor-like kinases in pollen tube tip integrity support this hypothesis. During pollen tube
388 growth through the female tissues, RALF4 and RALF19 peptides that are secreted from pollen
389 tubes act as ligands for ANX1/2 and BPS1/2 to promote tip growth, while RALF34 secreted from
390 the synergids displaces RALF4 and 19 from the receptors leading to subcellular changes that
391 result in pollen tube rupture (Ge et al., 2017).

392

393 **Calcium and NTA movement**

394 Our study revealed that an intact CaMBD facilitates the trafficking of NTA from the Golgi to the
395 filiform apparatus in response to a stimulus from the approaching pollen tube and that the
396 FER/LRE co-receptor is necessary for perceiving this stimulus. This result provides an intriguing
397 link to Ca^{2+} since the polar accumulation of NTA-GFP at the filiform apparatus region occurs in a
398 similar time frame to the FER/LRE-dependent $[Ca^{2+}]_{cyto}$ spiking in the synergids during pollen
399 tube reception (Denninger et al., 2014; Ngo et al., 2014). Subcellular Ca^{2+} spiking occurs in
400 plant responses to both biotic and abiotic external stimuli. Notably, $[Ca^{2+}]_{cyto}$ oscillations occur
401 during pollen tube-synergid interactions, egg-sperm interactions, and in biotrophic interactions
402 between plant cells and both beneficial and harmful microbes (reviewed in Chen et al., 2015). In
403 most cases, the mechanism for decoding $[Ca^{2+}]_{cyto}$ spikes into a cellular response is not known,
404 but Ca^{2+}-binding proteins such as calmodulin (CaM) and CaM-like proteins could play a role in
405 relaying Ca^{2+} signals (Chin and Means, 2000). In *nta-1* mutants, the $[Ca^{2+}]_{cyto}$ oscillations still
406 occur, but at a lower magnitude than in wild-type synergids, suggesting that NTA could be
407 involved in modulating Ca^{2+} flux (Ngo et al., 2014). The source of Ca^{2+} during these oscillations
408 is not known, but it is possible that NTA regulates Ca^{2+} channels to regulate the flow of Ca^{2+}ions
409 into or out of the apoplast near the filiform apparatus.

410

411 Ca^{2+} has also been linked to regulation of endomembrane trafficking (reviewed in Himschoot et
412 al., 2017). In animals, CaM plays a role in regulating vesicle tethering and fusion (Burgoyne and
413 Clague, 2003), and in plants CaM-like proteins are associated with endosomal populations
414 (Ruge et al., 2016). Thus, it is possible that the CaMBD in NTA is critical for the precise
415 targeting of NTA in response to pollen tube arrival. Another mechanism that has been proposed
416 for Ca^{2+} regulation of protein targeting is that electrostatic interactions between Ca^{2+} and anionic
417 phospholipids in specific domains of the plasma membrane regulate vesicle fusion and

418 differential recruitment of proteins to these domains (Simon et al., 2016; Platre et al., 2018). The
419 filiform apparatus of the synergids is distinctive from the plasma membrane in other parts of the
420 synergid and likely has a unique phospholipid composition that could play a role in recruiting
421 NTA to this domain. Whether NTA movement is a cause or consequence of $[Ca^{2+}]_{cyto}$ spiking
422 requires more live imaging experiments at a higher time resolution to determine if NTA
423 redistribution happens before or after the initiation of $[Ca^{2+}]_{cyto}$ spiking.
424
425 **Cell death and pollen tube reception**
426 MLOs were first discovered in barley as powdery mildew resistance genes (Buschges et al.,
427 1997). *mlo* mutants in both monocots and dicots are resistant to powdery mildew infection,
428 indicating that the MLO proteins are required for infection. These mutants also have ectopic cell
429 death, indicating that one function of MLO proteins is to negatively regulate cell death
430 (Panstruga, 2005). Pollen tube reception is catastrophic for both the pollen tube and the
431 receptive synergid cell: both cells die as a result of successful male-female signaling and
432 delivery of the male gametes. The timing of synergid degeneration remains under debate, with
433 some studies suggesting that it occurs upon pollen tube arrival at the synergid and others
434 concluding that it occurs concurrently with pollen tube rupture (Sandaklie-Nikolova et al., 2007;
435 Hamamura et al., 2011; Leydon et al., 2015). Our live imaging experiments with both NTA-GFP
436 and the subcellular compartment reporters suggest that the synergid cells are still alive and
437 regulating their secretory systems up to the point of pollen tube rupture. Given the function of
438 the “powdery mildew” members of the MLO gene family in preventing cell death, it is possible
439 that one role of NTA is to prevent early degeneration of the synergids. An interesting parallel
440 between powdery mildew infection and pollen tube reception is that, in both cases, an MLO
441 protein accumulates at the site of interaction with a tip-growing cell. In the powdery mildew
442 system, active transport of proteins and lipids to penetration site leads to membrane remodeling
443 and establishment of the extrahaustorial membrane which separates the plant cytoplasm from

444 the invading fungal hyphae (Huckelhoven and Panstruga, 2011). Although the relationship
445 between the arriving pollen tube and the filiform apparatus has not been established, it is
446 possible that similar reorganization occurs in the filiform apparatus during signaling with the
447 pollen tube. In both cases, perhaps an MLO protein is needed in these special membrane
448 regions to stabilize the cell and prevent precocious cell death. Our result that premature delivery
449 of NTA (in the NTA-MLO1^{CTerm} domain swap construct) to the filiform apparatus region of the
450 cell does not disrupt pollen tube reception is consistent with this hypothesis, since other
451 signaling processes occurring in the synergids during communication with the arriving pollen
452 tube would likely not be triggered by simply moving NTA to the filiform apparatus in the absence
453 of a pollen tube.
454
455 In this study, we showed that signals from an approaching pollen tube trigger the movement of
456 NTA out of the Golgi and to the filiform apparatus and that this redistribution is correlated with
457 pollen tube reception. However, filiform apparatus-localization of the NTA-MLO1^{CTerm} fusion
458 protein was able to complement the *nta-1* mutant phenotype, indicating that the final localization
459 of the NTA protein may be more important than the active trafficking from the Golgi. Future work
460 will focus on determining the mechanism through which NTA polarly accumulates at the filiform
461 apparatus and on identifying the signals from the pollen tube that lead to important subcellular
462 changes in the synergids during pollen tube reception.
463

Materials and methods

Plant materials and growth conditions

Arabidopsis thaliana lines expressing *NTA_{pro}::NTA-GFP*, *$MYB98_{pro}$::NTA-GFP*, *$MYB98_{pro}$::MLO1-GFP*,Golgi-associated marker (Man49-mCherry), ER-associated marker (SP-mCherry-HDEL), TGN-associated marker (SYP61-mCherry), peroxisome-associated marker (Peroxisome-mCherry) and recycling endosome-associated marker (mCherry-RabA1g), were generated and described in previous publications (Kessler et al., 2010; Liu et al., 2016; Jones et al., 2017; Jones et al., 2018). Pollen tube marker lines, *ACA9::DsRed* (Boisson-Dernier et al., 2008) and *Lat52::GFP* (Palanivelu and Preuss, 2006) were generously provided by Dr. Aurelien Boisson-Dernier and Dr. Ravi Palanivelu. *fer-1* seeds were provided by Dr. Ueli Grossniklaus and *lre-7* seeds were provided by Dr. Ravi Palanivelu. Seeds were sterilized and plated on ½-strength Murashige and Skoog (MS) plates. All plates were sealed and stratified at 4˚C for two days, and then transferred to the growth chamber (long day conditions, 16 h of light and 8 h of dark at 22˚C) for germination and growth. After 5-7 days, seedlings were transplanted to soil. Seeds from transformed lines were sterilized and plated on ½ MS plate with 20 mg/L hygromycin for selection of transgenic seedlings, which were then transplanted to soil and grown in long days.

Live Imaging of Pollination Using a Semi-*in vivo* Pollen Tube Guidance Assay

The semi-*in vivo* system of pollen tube reception was modified from (Palanivelu and Preuss, 2006). Approximately 150 µL of pollen germination media (5 mM KCl, 1 mM $MgSO_4$, 0.01% (w/v) H_3BO_3, 5 mM $CaCl_2$, 20% sucrose, 1.5% agarose, and adjusted pH to 7.5 with KOH) was poured into a Glass Bottom Culture Petri Dish (MatTek Corporation, P35G-1.0-20-C) and spread out using a pipette. Pistils were emasculated and 2 d later were hand pollinated with *ACA9::DsRed* or *Lat52::GFP* pollen and returned to the growth chamber. Approximately 1 h after pollination, pistils were removed from plants and placed on double sided tape on a glass

490 slide. Stigmas were cut using single-sided razor blade and placed on pollen germination media
491 using forceps. 8-10 ovules were arranged around the cut style and the petri dish was returned to
492 the growth chamber. After 4-6 h, pollen tubes grew through the stigma and style and emerged
493 near the ovules. Imaging commenced when the pollen tubes approached ovules. Time-lapse
494 images were acquired at 5 min intervals by spinning disk confocal microscopy using an Andor
495 Revolution XD platform with a Yokogawa CSU-X1-A1 scanner unit mounted on an Olympus IX-
496 83 microscope and a 20X/0.5 NA objective (Olympus). An Andor iXon Ultra 897BV EMCCD
497 camera was used to capture GFP fluorescence (488-nm excitation) and red fluorescent protein
498 (dsRed or mCherry) fluorescence (561-nm excitation).
499
500 For each experimental condition, at least 60 ovules were imaged over the time course from
501 pollen tube approaching the ovule to completion of pollen tube reception (pollen tube rupture to
502 release the sperm cells). Neighboring ovules that did not attract pollen tubes were imaged at the
503 same time and served as controls for photoxicity.
504
505 **Confocal laser scanning microscopy (CLSM)**
506 CLSM to examine MLO variant subcellular localization was performed on ovules dissected 2 d
507 after emasculation. FM4-64 staining was performed according to the protocol described in
508 (Jones et al., 2017). CLSM was done using either a Nikon A1Rsi inverted confocal microscope
509 according to (Yuan and Kessler, 2019) or a Leica SP8 upright confocal microscope according to
510 (Jones et al., 2017).
511
512 **Quantification of fluorescence signal intensity**
513 Two-channel images were adjusted for brightness and contrast using Fiji (Schindelin et al.,
514 2012). Then, they were input to NIS-Elements software (Ver. 5.02) to measure the fluorescence
515 signal intensity. A line that spanned from the chalazal end to the filiform apparatus end of the

synergid was used for the signal intensity measurements. For a more accurate representation of the total area of the synergid, signal intensities were recorded along the same length line at five parallel position within the synergid cell. Finally, all the measurement data were output as Excel files. Graphs and statistical analysis were performed with Prism software (www.graphpad.com).

Video processing

Images were filtered to remove the noise and cropped using Fiji (Version 2.0.0). QuickTime Player (Version 10.5) was used for movie editing and time-lapse analyses.

Cloning and Generation of Transgenic Lines

PCR amplification with PHUSION High-Fidelity Polymerase (NEB, M0535S) or Q5 High-Fidelity DNA Polymerase (NEB, M0419S) were used to generate the following constructs in this study. Genes were amplified with primers that had attB1 and attB2 sites for recombination via BP reaction into the Gateway-compatible entry vector pDONR207. Full-length NTA entry vectors used in this study was generated as described previously (Jones et al., 2017) . NTA truncations were amplified using NTA full-length entry vector as a template with forward primer NTA-FattB1 and the following reverse primers: NTA450-RattB2 and NTA481-RattB2 (See all primer sequences in Table S1). The NTA^{W458A} point mutation was generated using the same *NTA* template and amplifying two fragments of *NTA* with desired point mutations introduced into the primers: NTA-FattB1 + NTAW458A-R and NTAW458A-F + NTA-RattB2. The two fragments were purified and pasted together with overlaps using a PCR-pasting protocol. The NTA-MLO1^{CTerm} construct was generated using the full-length entry vectors of NTA and MLO1 used in previous study (Jones et al., 2017) as templates and amplifying two fragments of *NTA* and *MLO1* using the two pairs of primers: NTA-FattB1 +NTA-R19 and MLO1-F + MLO1-RattB2. The two fragments were purified and pasted together with overlaps using a PCR-pasting protocol. The NTA-MLO1^{CTerm}-RNIKCD construct was generated using the full-length expression vector of

MYB98$_{pro}$-NTA-MLO1^{CTerm}-GFP as template and amplifying two fragments with NTA-MLO1^{CTerm} and GFP-RNIKCD with five glycines as linker using the two pairs of primers: NTA-FattB1 + MLO1-Gly5-GFP-R and MLO1-Gly5-GFP-F + GFP-RNIKCD-RattB2. The two fragments were purified and pasted together with overlaps using a PCR-pasting protocol. The coding sequence from both truncations and the point mutation and the fusion sequences were fully sequenced in entry vectors. All entries were then recombined via LR reactions into the pMDC83 backbone with the MYB98$_{pro}$ (Muller et al., 2016) to drive expression of each NTA variant in synergid cells with a C-terminal GFP fusion.

For *nta-1* complementation assay and co-localization analyses, expression vectors were transformed into the *Agrobacterium tumefaciens* strain GV3101 and transformed into the *nta-1* mutant background or the Col-0 background (for co-localization combinations, Col-0 stably expressing the Golgi or TGN synergid secretory markers was used for transformation) via the floral-dip method (Bent, 2006). Stable transgenic lines were selected using their respective selections described above. Homozygous T2 lines were used in *nta-1* complementation assay and co-localization imaging in the synergid was done in a T1 analysis. The NTApro::NTA-GFP construct described in (Kessler et al., 2010) was introduced into the *lre-7* background by floral dip as described above.

nta-1 Complementation Assays

3-4 independent insertion lines for each construct were taken to the T2 generation and screened for homozygosity using fluorescence microscopy to ensure transgene expression in synergids of every ovule. Unfertilized vs. fertilized ovule counts from self-pollinated flowers were assessed in at least five plants of each insertion line and compared to *nta-1*, Wassilewskija (Ws-2; wildtype), and the previously published full-length NTA (MYB98$_{pro}$::NTA-GFP in *nta-1* background, (Jones et al., 2017). Ovule counts were statistically analyzed using Prism with

568 significance determined using a Student's *t*-test. Comparisons of the NTA variants were made
569 to full-length NTA and the *nta-1* mutant.
570
571 **Acknowledgements**
572 We thank Patrick Day for technical assistance and Rachel Flynn and Thomas Davis for helpful
573 discussions and comments on the manuscript. This work was supported by funds from NSF
574 IOS-1733865 to SAK, Purdue University Start-up funds to SAK, and a grant from the Oklahoma
575 Center for the Advancement of Science and Technology #PS14-008 to SAK. Spinning disk
576 confocal microscopy in the Staiger laboratory was supported, in part, by an award from the
577 Office of Science at the US Department of Energy, Physical Biosciences Program, under
578 contract number DE-FG02-09ER15526 to CJS.
579
580 **Author Contributions**
581 JY, YJ, DSJ, and SAK conceived and designed the experiments. JY, YJ, DSJ, NL, and WZ
582 performed the experiments. JY, YJ, DSJ, and SAK analyzed the data. JY, YJ, DSJ, and SAK
583 wrote the manuscript, and all authors revised and approved the final manuscript.
584
585 **Competing Interests**
586 The authors declare no competing interests.
587
588
589
590
591 **Figure Legends**
592 **Figure 1. NTA-GFP accumulates at the filiform apparatus as the pollen tube approaches.**
593 (A) Diagram of a mature *Arabidopsis thaliana* ovule and embryo sac, modified from Jones et al,

2018. CC, Central Cell; Syn, Synergid Cells; EC, Egg Cell; An, Antipodal cells; FA, Filiform Apparatus (B, C) Live imaging of pollen tube (PT) reception using NTA-GFP labeled synergids (green signal) and *ACA9::DsRed* pollen tubes (magenta signal). (B) Polar NTA-GFP accumulation at the filiform apparatus (FA) occurred in ovules that attracted a pollen tube (ovules with yellow stars), while polar NTA-GFP accumulation did not occur in ovules without pollen tube attraction (ovules with white stars). (C) Time-lapse imaging of NTA-GFP accumulation during pollen tube reception. (D) Quantification of NTA-GFP signal along the length of the synergid from chalazal end (0μm) to FA end (33μm) at 0min, 25min, 50min, 75min, and 100min timepoints, respectively. (E) 6 more examples of the quantification of NTA-GFP signal along the length of synergids after pollen tube arrival. (F) Quantification of the percentage of ovules with different NTA accumulation patterns under the same imaging conditions. Bars=50 μm (B and C).

Figure 2. The Golgi marker is randomly distributed throughout synergids during pollen tube reception. (A) NTA-GFP (green signal) and Golgi-mCherry signals (magenta signal) are evenly distributed along the length of the synergid and co-localized within synergid cells before pollen tube arrival. (B) After pollen tube arrival, NTA-GFP accumulated at the FA, but Golgi-mCherry did not accumulate at the FA. (C) Live imaging of Golgi-mCherry during reception of *Lat52::GFP* labeled pollen tubes. (D) Quantification of Golgi-mCherry signal along the length of synergids shown in (C) before and after pollen tube arrival. Bars=30μm (A-B), 50μm (C).

Figure 3. RabA1g endosomes polarly accumulate toward the filiform apparatus during pollen tube reception. (A) RabA1g-mCherry endosome marker (magenta signal) accumulates at the FA region in response to pollen tube arrival (ovule with yellow star). The ovule with no pollen tube attraction (white star) serves as a negative control imaged under the same conditions. (B) Higher magnification of the micropylar region of starred ovule in (red box in panel

620 A). (C) Timing of RabA1g-mCherry polar accumulation during pollen tube arrival. Bars=50μm.
621 (D) Quantification of RabA1g-mCherry signal along the length of synergids during pollen tube
622 reception. Synergid cell from chalazal end to filiform apparatus (FA) end was defined from 0 to
623 33 μm in length. (E) 6 more examples of the quantification of RabA1g-mCherry signal after
624 pollen tube arrival. (F) Quantification of ovule percentage with RabA1g endosome marker
625 throughout the synergids (gray bars) or with polar accumulation at or near the filiform apparatus
626 (black bars).
627
628 **Figure 4. Targeting of NTA to the filiform apparatus before pollen tube arrival is not toxic**
629 **to synergid cells.** (A-C) Localization patterns of MYB98 promoter driven MLO-GFP variants
630 (green signal) in synergids of mature virgin ovules stained with FM4-64 (magenta signal) to reveal
631 the outline of the synergid and the filiform apparatus (FA, diffuse magenta signal). Bars = 10 μm.
632 (D) Quantification of the GFP intensity of the MLO variants in A-C along the length of the synergids.
633 (E) Percentage of ovules showing MLO-GFP signal throughout the synergids (100% of length), in
634 the FA only (20% of length) and the region surrounding and including the FA (40% of length). (F)
635 Scatter plot of unfertilized ovule percentages in homozygous plants of pMYB98::MLO-GFP in *nta-*
636 *1* mutants to assess the ability of the MLO-GFP constructs to complement *nta-1*. WS,
637 Wassilewskija. Significance was determined by a Student's *t*-test (****, $P < 0.0001$; *, $P = 0.0281$;
638 and ns, $P = 0.2020$).
639
640 **Figure 5. Analysis of NTA variants expressed in synergids of *nta-1*.** (A) Alignment of MLO1
641 and NTA C-terminal domains after the seventh membrane span. Red bars highlight the CaMBD;
642 W458A and Δ481 indicate the point mutation in NTA and the deletion point, respectively ; a.a.,
643 amino acid. (B-D) NTA (variant)-GFP (green) distribution in synergid cells of unfertilized ovules
644 stained with FM4-64 (magenta signal). Bar = 10 μm. (E) Complementation analysis of NTA
645 variants in T2 plants homozygous for $MYB98_{pro}$::NTA(variant)-GFP constructs in *nta-1* mutants.

Adjusted P values from a Student's *t*-test are as follows: **** indicates $P < 0.0001$; *** indicates $P = 0.001$ to 0.0001; and ns indicates $P > 0.05$.

Figure 6. A point mutation in the CaMBD (NTA^{W458A}) affects filiform apparatus accumulation of NTA and pollen tube reception. (A) NTA^{W458A}-GFP has 3 different localization patterns in response to PT arrival under semi *in-vivo* conditions. Bar=50 μm (B) Quantification of GFP signal intensity in NTA^{W458A} synergids during pollen tube reception. (C) Analysis of NTA^{W458A}-GFP distribution patterns in ovules with successful (PT bursting) and unsuccessful (no PT or PT overgrowth (PT OG)) pollen tube reception.

Figure 7. Subcellular dynamics in synergids during pollen tube reception. (A) Pollination using a semi-*in vivo* pollen tube guidance assay. (B) Before pollen tube arrival, NTA is in a Golgi-associated compartment and RabA1g endosomes are distributed throughout the synergids. (C) As a pollen tube arrives, NTA and RabA1g endosomes move toward the filiform apparatus (FA). NTA accumulation is dependent on signaling from the FER receptor like kinase, which acts in a complex with LRE. Abbreviations: CC, Central Cell; Syn, Synergid cells; EC, Egg Cell; An, Antipodal cells; nuc, Nucleus; FA, Filiform Apparatus.

Supplemental Materials

Supplementary figure 1. NTA-GFP does not polarly accumulate at the filiform apparatus in synergids without pollen tube attraction.

Supplementary figure 2. Peroxisomes do not exhibit polar accumulation at the FA during pollen tube reception.

Supplementary figure 3. Trans-Golgi marker distribution in synergids does not change in response to pollen tube reception.

672 **Supplementary figure 4.** ER marker distribution in synergids does not change in response to
673 pollen tube reception.
674 **Supplementary figure 5**. Additional examples of the polar accumulation of RabA1g endosomes
675 during pollen tube reception.
676 **Supplementary figure 6.** NTA^{W458A} co-localizes with Golgi marker in synergid cells before pollen
677 tube arrival.
678 **Supplementary figure 7**. NTA-GFP polar accumulation requires FER and LRE.
679
680 **Supplemental Movies**
681 **Supplementary movie 1.** NTA-GFP (green signal) redistributes to filiform apparatus region as
682 ACA9::DsRed labeled pollen tube (magenta signal) approaches.
683 **Supplementary movie 2.** NTA-GFP (green signal) redistributes to filiform apparatus region
684 during pollen tube reception (GFP channel only, same movie as S1).
685 **Supplementary movie 3.** Golgi-mCherry signals (magenta signal) are evenly distributed along
686 the length of the synergid as Lat52::GFP labeled pollen tube (green signal) approaches.
687 **Supplementary movie 4.** Golgi-mCherry signals (magenta signal) are evenly distributed along
688 the length of the synergid during pollen tube reception (mCherry channel only, same movie as
689 S3).
690 **Supplementary movie 5.** The trans-Golgi marker SYP61-mCherry (magenta signal) is localized
691 toward the micropyle region of synergid cells both before and after pollen tube (green signal)
692 arrival.
693 **Supplementary movie 6.** The trans-Golgi marker SYP61-mCherry (magenta signal) is localized
694 toward the micropyle region of synergid cells during pollen tube reception (mCherry channel
695 only, same movie as S5).
696 **Supplementary movie 7.** Before and after pollen tube (green signal) arrival, the ER marker SP-
697 mCherry-HDEL (magenta signal) is distributed throughout synergid cells.

Supplementary movie 8. The ER marker SP-mCherry-HDEL (magenta signal) is distributed throughout synergid cells (mCherry channel only, same movie as S7).

Supplementary movie 9. The peroxisome marker mCherry-SLK (magenta signal) does not redistribute to the filiform apparatus region after pollen tube (green signal) arrival.

Supplementary movie 10. The peroxisome marker mCherry-SLK (magenta signal) does not redistribute to the filiform apparatus region during pollen tube reception (mCherry channel only, same movie as S9).

Supplementary movie 11. RabA1g-mCherry endosome marker (magenta signal) accumulates at the filiform apparatus region in response to pollen tube (green signal) arrival.

References

Arazi, T., Baum, G., Snedden, W.A., Shelp, B.J., and Fromm, H. (1995). Molecular and Biochemical-Analysis of Calmodulin Interactions with the Calmodulin-Binding Domain of Plant Glutamate-Decarboxylase. Plant Physiology **108,** 551-561.

Bent, A. (2006). Arabidopsis thaliana Floral Dip Transformation Method. In Methods in Molecular Biology, K. Wang, ed (Totowa, NJ: Humana Press Inc.

Boisson-Dernier, A., Frietsch, S., Kim, T.H., Dizon, M.B., and Schroeder, J.I. (2008). The peroxin loss-of-function mutation abstinence by mutual consent disrupts male-female gametophyte recognition. Curr Biol **18,** 63-68.

Burgoyne, R.D., and Clague, M.J. (2003). Calcium and calmodulin in membrane fusion. Biochim Biophys Acta **1641,** 137-143.

Buschges, R., Hollricher, K., Panstruga, R., Simons, G., Wolter, M., Frijters, A., van Daelen, R., van der Lee, T., Diergaarde, P., Groenendijk, J., Topsch, S., Vos, P., Salamini, F., and Schulze-Lefert, P. (1997). The barley Mlo gene: a novel control element of plant pathogen resistance. Cell **88,** 695-705.

Capron, A., Gourgues, M., Neiva, L.S., Faure, J.E., Berger, F., Pagnussat, G., Krishnan, A., Alvarez-Mejia, C., Vielle-Calzada, J.P., Lee, Y.R., Liu, B., and Sundaresan, V. (2008). Maternal Control of Male-Gamete Delivery in Arabidopsis Involves a Putative GPI-Anchored Protein Encoded by the LORELEI Gene. Plant Cell **20,** 3038-3049.

Chen, J., Gutjahr, C., Bleckmann, A., and Dresselhaus, T. (2015). Calcium signaling during reproduction and biotrophic fungal interactions in plants. Mol Plant **8,** 595-611.

Chin, D., and Means, A.R. (2000). Calmodulin: a prototypical calcium sensor. Trends Cell Biol **10,** 322-328.

Denninger, P., Bleckmann, A., Lausser, A., Vogler, F., Ott, T., Ehrhardt, D.W., Frommer, W.B., Sprunck, S., Dresselhaus, T., and Grossmann, G. (2014). Male-female communication triggers calcium signatures during fertilization in Arabidopsis. Nature communications **5,** 4645.

Devoto, A., Piffanelli, P., Nilsson, I., Wallin, E., Panstruga, R., von Heijne, G., and Schulze-Lefert, P. (1999). Topology, subcellular localization, and sequence diversity of the Mlo family in plants. J Biol Chem **274,** 34993-35004.

Devoto, A., Hartmann, H.A., Piffanelli, P., Elliott, C., Simmons, C., Taramino, G., Goh, C.S., Cohen, F.E., Emerson, B.C., Schulze-Lefert, P., and Panstruga, R. (2003). Molecular phylogeny and evolution of the plant-specific seven-transmembrane MLO family. J Mol Evol **56,** 77-88.

Drews, G.N., and Yadegari, R. (2002). Development and function of the angiosperm female gametophyte. Annu Rev Genet **36,** 99-124.

Escobar-Restrepo, J.M., Huck, N., Kessler, S., Gagliardini, V., Gheyselinck, J., Yang, W.C., and Grossniklaus, U. (2007). The FERONIA receptor-like kinase mediates male-female interactions during pollen tube reception. Science **317,** 656-660.

Gao, C., Yu, C.K., Qu, S., San, M.W., Li, K.Y., Lo, S.W., and Jiang, L. (2012). The Golgi-localized Arabidopsis endomembrane protein12 contains both endoplasmic reticulum export and Golgi retention signals at its C terminus. Plant Cell **24,** 2086-2104.

Ge, Z., Bergonci, T., Zhao, Y., Zou, Y., Du, S., Liu, M.C., Luo, X., Ruan, H., Garcia-Valencia, L.E., Zhong, S., Hou, S., Huang, Q., Lai, L., Moura, D.S., Gu, H., Dong, J., Wu, H.M., Dresselhaus, T., Xiao, J., Cheung, A.Y., and Qu, L.J. (2017). Arabidopsis pollen tube integrity and sperm release are regulated by RALF-mediated signaling. Science **358,** 1596-1600.

Geldner, N., Denervaud-Tendon, V., Hyman, D.L., Mayer, U., Stierhof, Y.D., and Chory, J. (2009). Rapid, combinatorial analysis of membrane compartments in intact plants with a multicolor marker set. Plant J **59,** 169-178.

Hamamura, Y., Nagahara, S., and Higashiyama, T. (2012). Double fertilization on the move. Curr Opin Plant Biol **15,** 70-77.

Hamamura, Y., Nishimaki, M., Takeuchi, H., Geitmann, A., Kurihara, D., and Higashiyama, T. (2014). Live imaging of calcium spikes during double fertilization in Arabidopsis. Nat Commun **5,** 4722.

Hamamura, Y., Saito, C., Awai, C., Kurihara, D., Miyawaki, A., Nakagawa, T., Kanaoka, M.M., Sasaki, N., Nakano, A., Berger, F., and Higashiyama, T. (2011). Live-cell imaging reveals the dynamics of two sperm cells during double fertilization in Arabidopsis thaliana. Curr Biol **21,** 497-502.

Himschoot, E., Pleskot, R., Van Damme, D., and Vanneste, S. (2017). The ins and outs of Ca(2+) in plant endomembrane trafficking. Curr Opin Plant Biol **40,** 131-137.

Huang, B.-Q., and Russell, S.D. (1992). Female Germ Unit: Organization, Isolation, and Function **140,** 233-293.

Huck, N., Moore, J.M., Federer, M., and Grossniklaus, U. (2003). The Arabidopsis mutant feronia disrupts the female gametophytic control of pollen tube reception. Development **130,** 2149-2159.

Huckelhoven, R., and Panstruga, R. (2011). Cell biology of the plant-powdery mildew interaction. Curr Opin Plant Biol **14,** 738-746.

Iwano, M., Ngo, Q.A., Entani, T., Shiba, H., Nagai, T., Miyawaki, A., Isogai, A., Grossniklaus, U., and Takayama, S. (2012). Cytoplasmic Ca2+ changes dynamically during the interaction of the pollen tube with synergid cells. Development **139,** 4202-4209.

Johnson, M.A., Harper, J.F., and Palanivelu, R. (2019). A Fruitful Journey: Pollen Tube Navigation from Germination to Fertilization. Annu Rev Plant Biol.

Jones, D.S., and Kessler, S.A. (2017). Cell type-dependent localization of MLO proteins. Plant Signal Behav **12**.

Jones, D.S., Yuan, J., Smith, B.E., Willoughby, A.C., Kumimoto, E.L., and Kessler, S.A. (2017). MILDEW RESISTANCE LOCUS O Function in Pollen Tube Reception Is Linked to Its Oligomerization and Subcellular Distribution. Plant Physiol **175,** 172-185.

Jones, D.S., Liu, X., Willoughby, A.C., Smith, B.E., Palanivelu, R., and Kessler, S.A. (2018). Cellular distribution of secretory pathway markers in the haploid synergid cells of Arabidopsis thaliana. Plant J **94,** 192-202.

Kessler, S.A., and Grossniklaus, U. (2011). She's the boss: signaling in pollen tube reception. Curr Opin Plant Biol **14,** 622-627.

Kessler, S.A., Shimosato-Asano, H., Keinath, N.F., Wuest, S.E., Ingram, G., Panstruga, R., and Grossniklaus, U. (2010). Conserved molecular components for pollen tube reception and fungal invasion. Science **330,** 968-971.

Kim, M.C., Panstruga, R., Elliott, C., Muller, J., Devoto, A., Yoon, H.W., Park, H.C., Cho, M.J., and Schulze-Lefert, P. (2002a). Calmodulin interacts with MLO protein to regulate defence against mildew in barley. Nature **416,** 447-451.

Kim, M.C., Lee, S.H., Kim, J.K., Chun, H.J., Choi, M.S., Chung, W.S., Moon, B.C., Kang, C.H., Park, C.Y., Yoo, J.H., Kang, Y.H., Koo, S.C., Koo, Y.D., Jung, J.C., Kim, S.T., Schulze-Lefert, P., Lee, S.Y., and Cho, M.J. (2002b). Mlo, a modulator of plant defense and cell death, is a novel calmodulin-binding protein. Isolation and characterization of a rice Mlo homologue. J Biol Chem **277,** 19304-19314.

Kusch, S., Pesch, L., and Panstruga, R. (2016). Comprehensive Phylogenetic Analysis Sheds Light on the Diversity and Origin of the MLO Family of Integral Membrane Proteins. Genome Biol Evol **8,** 878-895.

Leshem, Y., Johnson, C., and Sundaresan, V. (2013). Pollen tube entry into the synergid cell of Arabidopsis is observed at a site distinct from the filiform apparatus. Plant reproduction **26,** 93-99.

Leydon, A.R., Tsukamoto, T., Dunatunga, D., Qin, Y., Johnson, M.A., and Palanivelu, R. (2015). Pollen Tube Discharge Completes the Process of Synergid Degeneration That Is Initiated by Pollen Tube-Synergid Interaction in Arabidopsis. Plant Physiol **169,** 485-496.

Li, C., Yeh, F.L., Cheung, A.Y., Duan, Q., Kita, D., Liu, M.C., Maman, J., Luu, E.J., Wu, B.W., Gates, L., Jalal, M., Kwong, A., Carpenter, H., and Wu, H.M. (2015). Glycosylphosphatidylinositol-anchored proteins as chaperones and co-receptors for FERONIA receptor kinase signaling in Arabidopsis. Elife **4**.

Lindner, H., Kessler, S.A., Müller, L.M., Shimosato-Asano, H., Boisson-Dernier, A., and Grossniklaus, U. (2015). TURAN and EVAN mediate pollen tube reception in Arabidopsis synergids through protein glycosylation. PLoS Biol **13,** e1002139.

Liu, X., Castro, C., Wang, Y., Noble, J., Ponvert, N., Bundy, M., Hoel, C., Shpak, E., and Palanivelu, R. (2016). The Role of LORELEI in Pollen Tube Reception at the Interface of the Synergid Cell and Pollen Tube Requires the Modified Eight-Cysteine Motif and the Receptor-Like Kinase FERONIA. Plant Cell **28,** 1035-1052.

Mansfield, S.G., Briarty, L.G., and Erni, S. (1991). Early embryogenesis in Arabidopsis thaliana. I. The mature embryo sac. Canadian Journal of Botany **69,** 447-460.

Muller, L.M., Lindner, H., Pires, N.D., Gagliardini, V., and Grossniklaus, U. (2016). A subunit of the oligosaccharyltransferase complex is required for interspecific gametophyte recognition in Arabidopsis. Nat Commun **7,** 10826.

Naramoto, S. (2017). Polar transport in plants mediated by membrane transporters: focus on mechanisms of polar auxin transport. Curr Opin Plant Biol **40,** 8-14.

Ngo, Q.A., Vogler, H., Lituiev, D.S., Nestorova, A., and Grossniklaus, U. (2014). A Calcium Dialog Mediated by the FERONIA Signal Transduction Pathway Controls Plant Sperm Delivery. Dev Cell **29,** 491-500.

Okuda, S., Tsutsui, H., Shiina, K., Sprunck, S., Takeuchi, H., Yui, R., Kasahara, R.D., Hamamura, Y., Mizukami, A., Susaki, D., Kawano, N., Sakakibara, T., Namiki, S.,

Itoh, K., Otsuka, K., Matsuzaki, M., Nozaki, H., Kuroiwa, T., Nakano, A., Kanaoka, M.M., Dresselhaus, T., Sasaki, N., and Higashiyama, T. (2009). Defensin-like polypeptide LUREs are pollen tube attractants secreted from synergid cells. Nature **458,** 357-361.

Palanivelu, R., and Preuss, D. (2006). Distinct short-range ovule signals attract or repel Arabidopsis thaliana pollen tubes in vitro. BMC Plant Biol **6,** 7.

Panstruga, R. (2005). Serpentine plant MLO proteins as entry portals for powdery mildew fungi. Biochem Soc Trans **33,** 389-392.

Petrasek, J., Mravec, J., Bouchard, R., Blakeslee, J.J., Abas, M., Seifertova, D., Wisniewska, J., Tadele, Z., Kubes, M., Covanova, M., Dhonukshe, P., Skupa, P., Benkova, E., Perry, L., Krecek, P., Lee, O.R., Fink, G.R., Geisler, M., Murphy, A.S., Luschnig, C., Zazimalova, E., and Friml, J. (2006). PIN proteins perform a rate-limiting function in cellular auxin efflux. Science **312,** 914-918.

Platre, M.P., Noack, L.C., Doumane, M., Bayle, V., Simon, M.L.A., Maneta-Peyret, L., Fouillen, L., Stanislas, T., Armengot, L., Pejchar, P., Caillaud, M.C., Potocky, M., Copic, A., Moreau, P., and Jaillais, Y. (2018). A Combinatorial Lipid Code Shapes the Electrostatic Landscape of Plant Endomembranes. Dev Cell **45,** 465-480 e411.

Rotman, N., Rozier, F., Boavida, L., Dumas, C., Berger, F., and Faure, J.E. (2003). Female control of male gamete delivery during fertilization in Arabidopsis thaliana. Curr Biol **13,** 432-436.

Ruge, H., Flosdorff, S., Ebersberger, I., Chigri, F., and Vothknecht, U.C. (2016). The calmodulin-like proteins AtCML4 and AtCML5 are single-pass membrane proteins targeted to the endomembrane system by an N-terminal signal anchor sequence. J Exp Bot **67,** 3985-3996.

Salanenka, Y., Verstraeten, I., Lofke, C., Tabata, K., Naramoto, S., Glanc, M., and Friml, J. (2018). Gibberellin DELLA signaling targets the retromer complex to redirect protein trafficking to the plasma membrane. Proc Natl Acad Sci U S A **115,** 3716-3721.

Sandaklie-Nikolova, L., Palanivelu, R., King, E.J., Copenhaver, G.P., and Drews, G.N. (2007). Synergid cell death in Arabidopsis is triggered following direct interaction with the pollen tube. Plant Physiol **144,** 1753-1762.

Schindelin, J., Arganda-Carreras, I., Frise, E., Kaynig, V., Longair, M., Pietzsch, T., Preibisch, S., Rueden, C., Saalfeld, S., Schmid, B., Tinevez, J.Y., White, D.J., Hartenstein, V., Eliceiri, K., Tomancak, P., and Cardona, A. (2012). Fiji: an open-source platform for biological-image analysis. Nat Methods **9,** 676-682.

Simon, M.L., Platre, M.P., Marques-Bueno, M.M., Armengot, L., Stanislas, T., Bayle, V., Caillaud, M.C., and Jaillais, Y. (2016). A PtdIns(4)P-driven electrostatic field controls cell membrane identity and signalling in plants. Nat Plants **2,** 16089.

Sprunck, S., Rademacher, S., Vogler, F., Gheyselinck, J., Grossniklaus, U., and Dresselhaus, T. (2012). Egg cell-secreted EC1 triggers sperm cell activation during double fertilization. Science **338,** 1093-1097.

Stoorvogel, W., Strous, G.J., Geuze, H.J., Oorschot, V., and Schwartz, A.L. (1991). Late endosomes derive from early endosomes by maturation. Cell **65,** 417-427.

Takeuchi, H., and Higashiyama, T. (2016). Tip-localized receptors control pollen tube growth and LURE sensing in Arabidopsis. Nature **531,** 245-248.

Viotti, C., Bubeck, J., Stierhof, Y.D., Krebs, M., Langhans, M., van den Berg, W., van Dongen, W., Richter, S., Geldner, N., Takano, J., Jurgens, G., de Vries, S.C., Robinson, D.G., and Schumacher, K. (2010). Endocytic and secretory traffic in Arabidopsis merge in the trans-Golgi network/early endosome, an independent and highly dynamic organelle. Plant Cell **22,** 1344-1357.

885 **Wang, T., Liang, L., Xue, Y., Jia, P.F., Chen, W., Zhang, M.X., Wang, Y.C., Li, H.J., and**
886 **Yang, W.C.** (2016). A receptor heteromer mediates the male perception of female
887 attractants in plants. Nature **531,** 241-244.
888 **Yamada, M., Miyawaki, A., Saito, K., Nakajima, T., Yamamoto-Hino, M., Ryo, Y., Furuichi,**
889 **T., and Mikoshiba, K.** (1995). The calmodulin-binding domain in the mouse type 1
890 inositol 1,4,5-trisphosphate receptor. Biochem J **308 (Pt 1),** 83-88.
891 **Yang, T., and Poovaiah, B.** (2003). Calcium/calmodulin-mediated signal network in plants.
892 Trends in plant science **8,** 505-512.
893 **Yuan, J., and Kessler, S.A.** (2019). A genome-wide association study reveals a novel regulator
894 of ovule number and fertility in Arabidopsis thaliana. PLoS Genet **15,** e1007934.
895

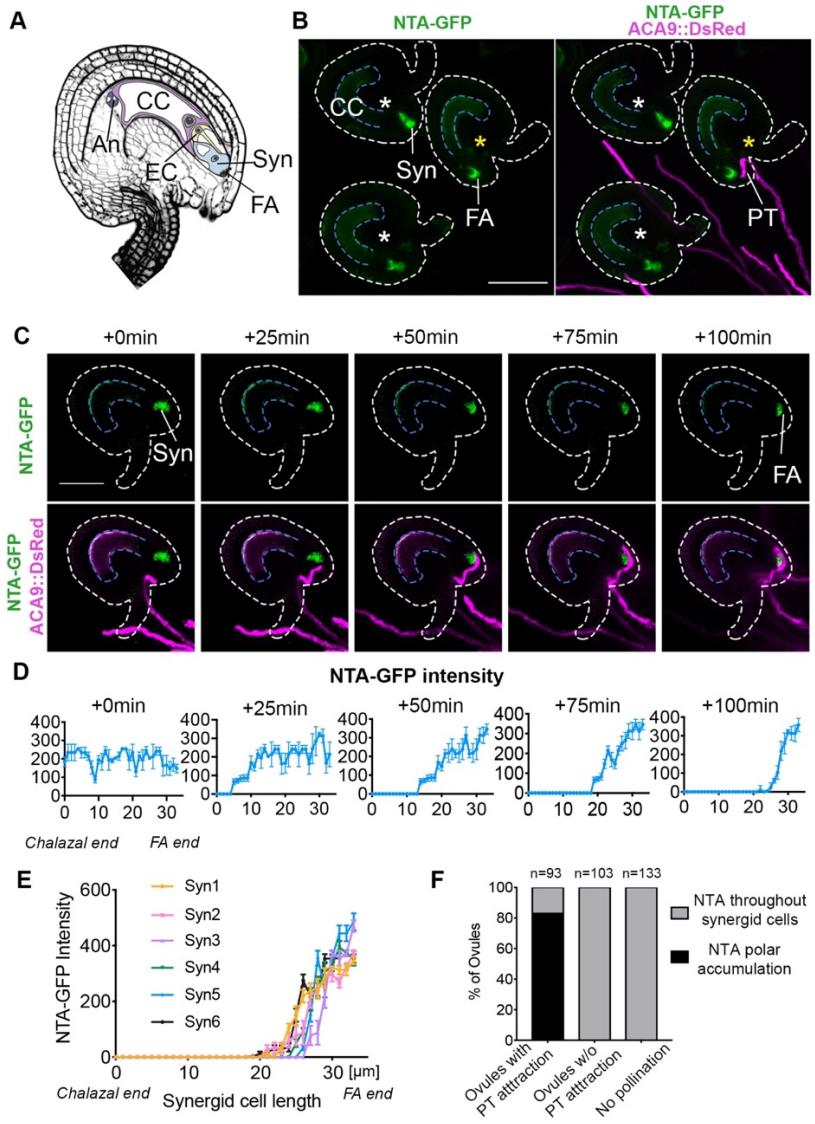

Figure 1. NTA-GFP accumulates at the filiform apparatus as the pollen tube approaches. (A) Diagram of a mature *Arabidopsis thaliana* ovule and embryo sac, modified from Jones et al, 2018. CC, Central Cell; Syn, Synergid Cells; EC, Egg Cell; An, Antipodal cells; FA, Filiform Apparatus (B, C) Live imaging of pollen tube (PT) reception using NTA-GFP labeled synergids (green signal) and ACA9::DsRed pollen tubes (magenta signal). (B) Polar NTA-GFP accumulation at the filiform apparatus (FA) occurred in ovules that attracted a pollen tube (ovules with yellow stars), while polar NTA-GFP accumulation did not occur in ovules without pollen tube attraction (ovules with white stars). (C) Time-lapse imaging of NTA-GFP accumulation during pollen tube reception. (D) Quantification of NTA-GFP signal along the length of the synergid from chalazal end (0μm) to FA end (33μm) at 0min, 25min, 50min, 75min, and 100min timepoints, respectively. (E) 6 more examples of the quantification of NTA-GFP signal along the length of synergids after pollen tube arrival. (F) Quantification of the percentage of ovules with different NTA accumulation patterns under the same imaging conditions. Bars=50 μm (B and C).

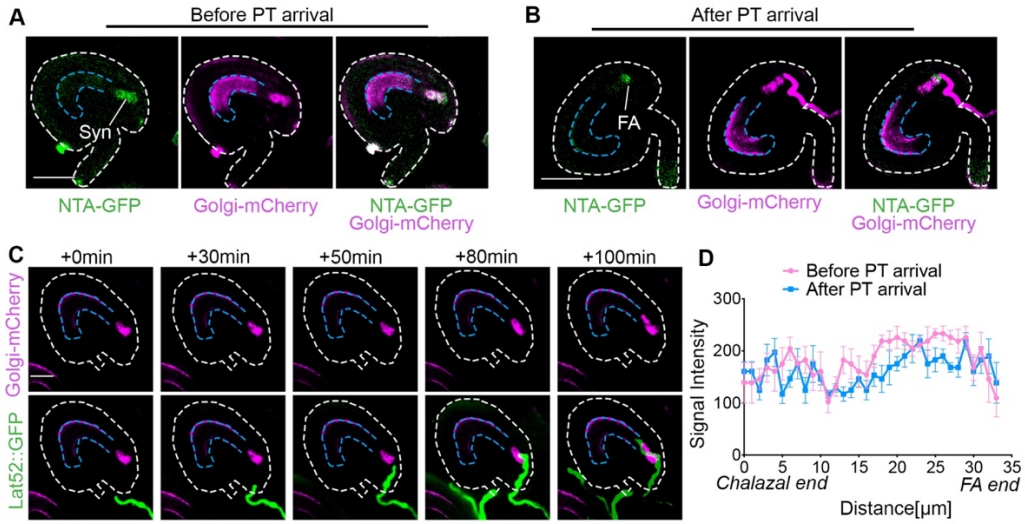

Figure 2. A Golgi marker is randomly distributed throughout synergids during pollen tube reception. (A) NTA-GFP (green signal) and Golgi-mCherry signals (magenta signal) are evenly distributed along the length of the synergid and co-localized within synergid cells before pollen tube arrival. (B) After pollen tube arrival, NTA-GFP accumulated at the FA, but Golgi-mCherry did not accumulate at the FA. (C) Live imaging of Golgi-mCherry during reception of Lat52::GFP labeled pollen tubes. (D) Quantification of Golgi-mCherry signal along the length of synergids shown in (C) before and after pollen tube arrival. Bars=30μm (A-B), 50μm (C).

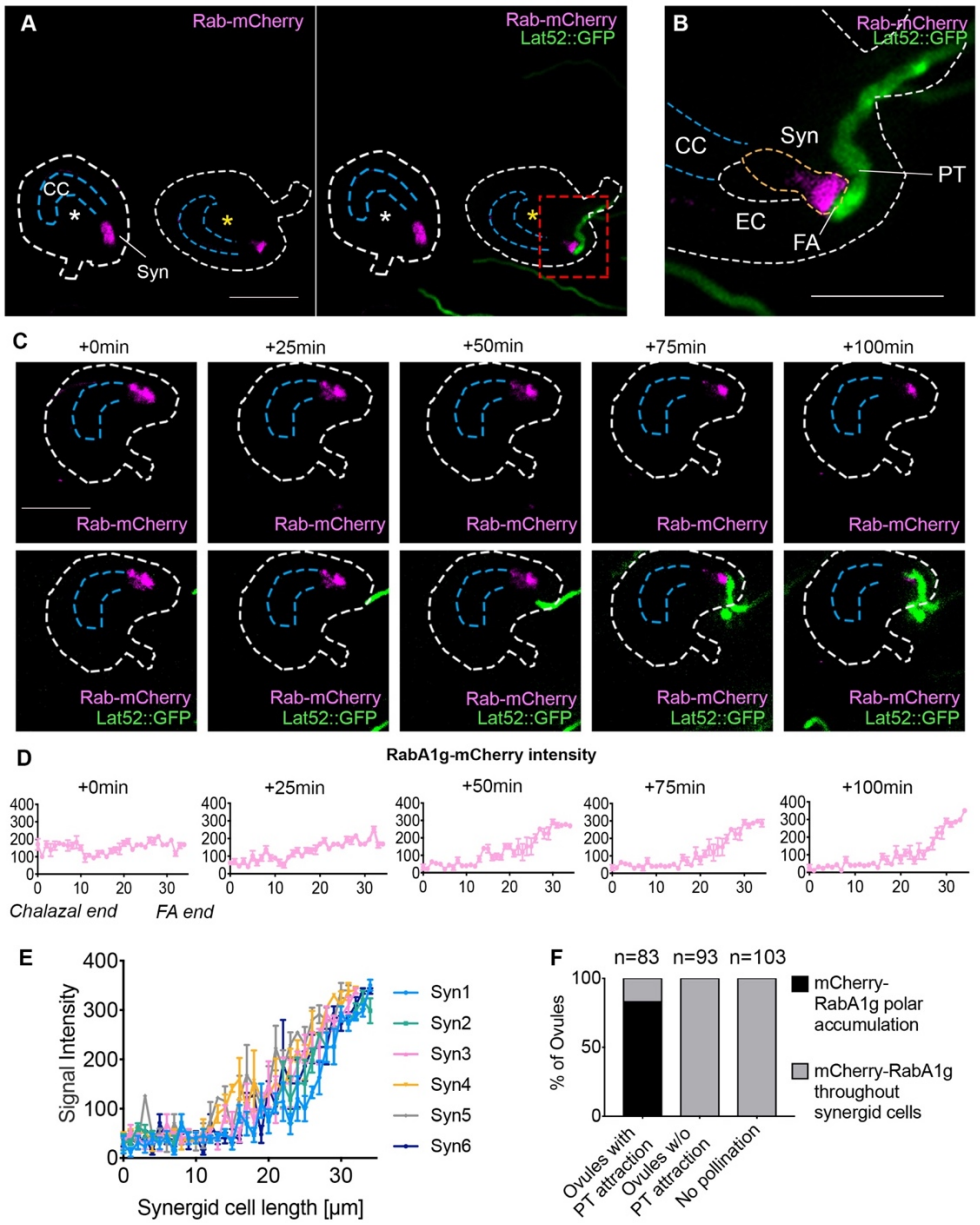

Figure 3. RabA1g endosomes polarly accumulate toward the filiform apparatus during pollen tube reception. (A) RabA1g-mCherry endosome marker (magenta signal) accumulates at the FA region in response to pollen tube arrival (ovule with yellow star). The ovule with no pollen tube attraction (white star) serves as a negative control imaged under the same conditions. (B) Higher magnification of the micropylar region of starred ovule in (red box in panel A). (C) Timing of RabA1g-mCherry polar accumulation during pollen tube arrival. Bars=50μm. (D) Quantification of RabA1g-mCherry signal along the length of synergids during pollen tube reception. Synergid cell from chalazal end to filiform apparatus (FA) end was defined from 0 to 33 μm in length. (E) 6 more examples of the quantification of RabA1g-mCherry signal after pollen tube arrival. (F) Quantification of ovule percentage with RabA1g endosome marker throughout the synergids (gray bars) or with polar accumulation at or near the filiform apparatus (black bars).

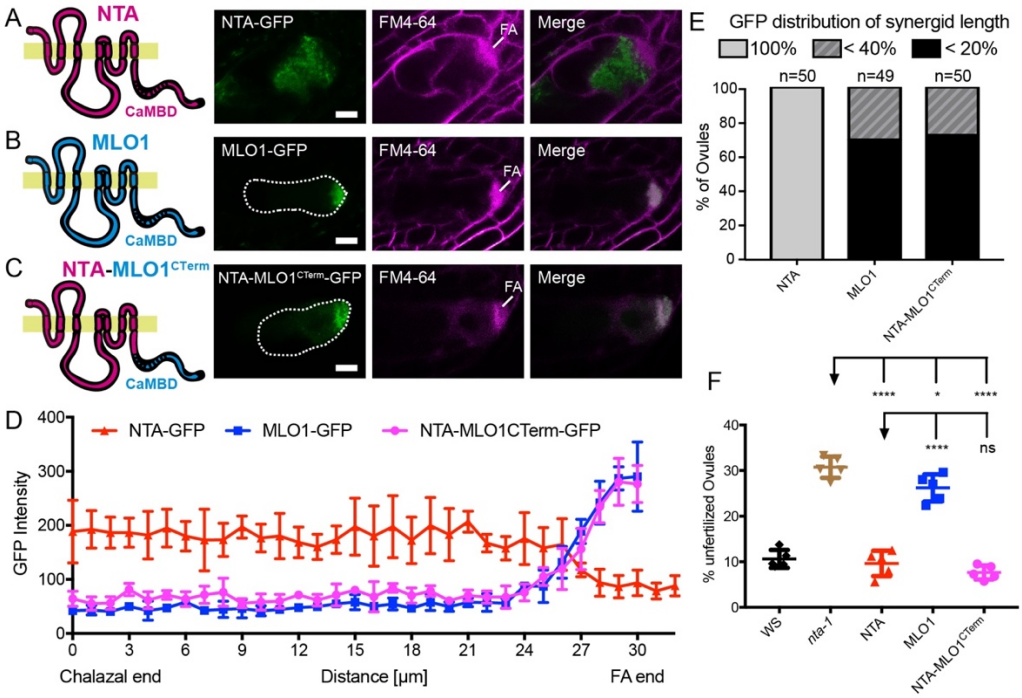

Figure 4. Targeting of NTA to the filiform apparatus before pollen tube arrival is not toxic to synergid cells. (A-C) Localization patterns of MYB98 promoter driven MLO-GFP variants (green signal) in synergids of mature virgin ovules stained with FM4-64 (magenta signal) to reveal the outline of the synergid and the filiform apparatus (FA, diffuse magenta signal). Bars = 10 µm. (D) Quantification of the GFP intensity of the MLO variants in A-C along the length of the synergids. (E) Percentage of ovules showing MLO-GFP signal throughout the synergids (100% of length), in the FA only (20% of length) and the region surrounding and including the FA (40% of length). (F) Scatter plot of unfertilized ovule percentages in homozygous plants of pMYB98::MLO-GFP in *nta-1* mutants to assess the ability of the MLO-GFP constructs to complement *nta-1*. WS, Wassilewskija. Significance was determined by a Student's *t*-test (****, $P < 0.0001$; *, $P = 0.0281$; and ns, $P = 0.2020$).

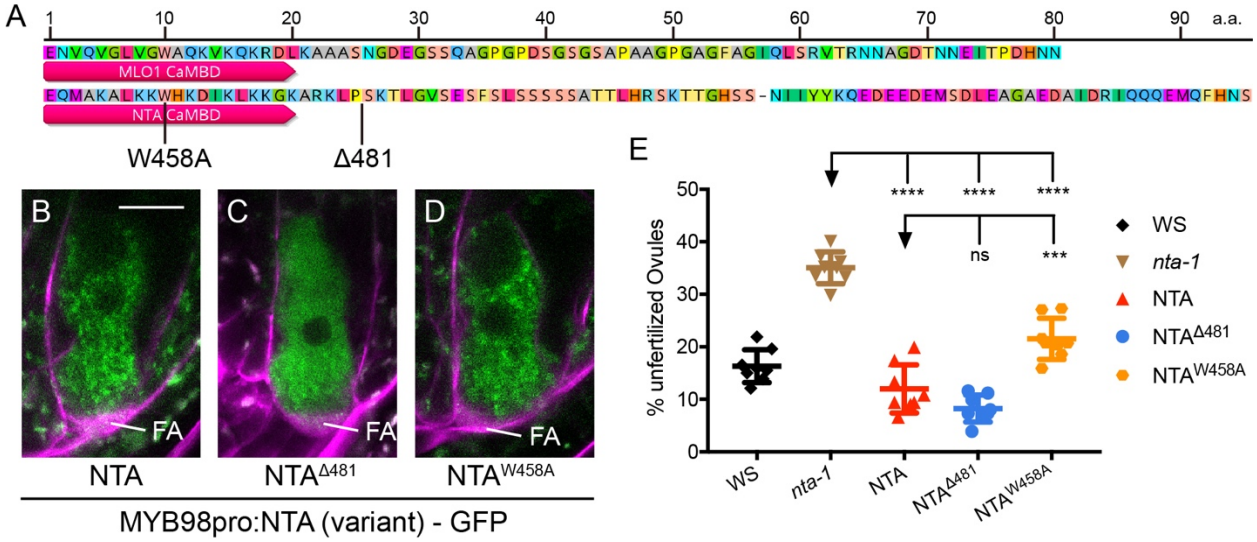

Figure 5. Disruption of the CaMBD affects NTA localization and function. (A) Alignment of MLO1 and NTA C-terminal domains after the seventh membrane span. Red bars highlight the CaMBD; W458A and Δ481 indicate the point mutation in NTA and the deletion point, respectively ; a.a., amino acid. (B-D) NTA (variant)-GFP (green) distribution in synergid cells of unfertilized ovules stained with FM4-64 (magenta signal). Bar = 10 µm. (E) Complementation analysis of NTA variants in T2 plants homozygous for $MYB98_{pro}$::NTA(variant)-GFP constructs in *nta-1* mutants. Adjusted P values from a Student's *t*-test are as follows: **** indicates $P < 0.0001$; *** indicates $P = 0.001$ to 0.0001; and ns indicates $P > 0.05$.

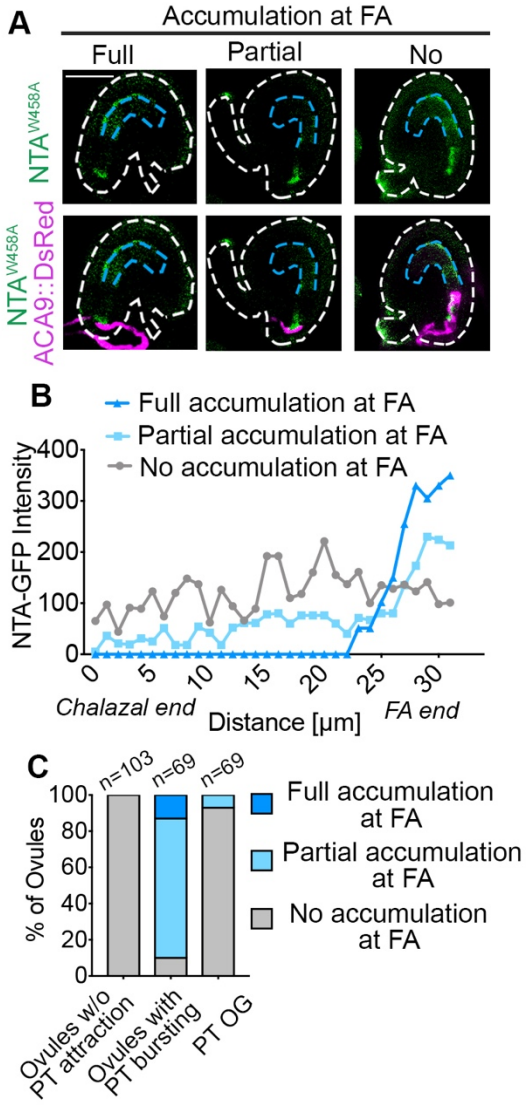

Figure 6. A point mutation in the CaMBD (NTA^{W458A}) affects filiform apparatus accumulation of NTA and pollen tube reception. (A) NTA^{W458A}-GFP has 3 different localization patterns in response to PT arrival under semi *in-vivo* conditions. Bar=50 µm (B) Quantification of GFP signal intensity in NTA^{W458A} synergids during pollen tube reception. (C) Analysis of NTA^{W458A}-GFP distribution patterns in ovules with successful (PT bursting) and unsuccessful (no PT or PT overgrowth (PT OG)) pollen tube reception.

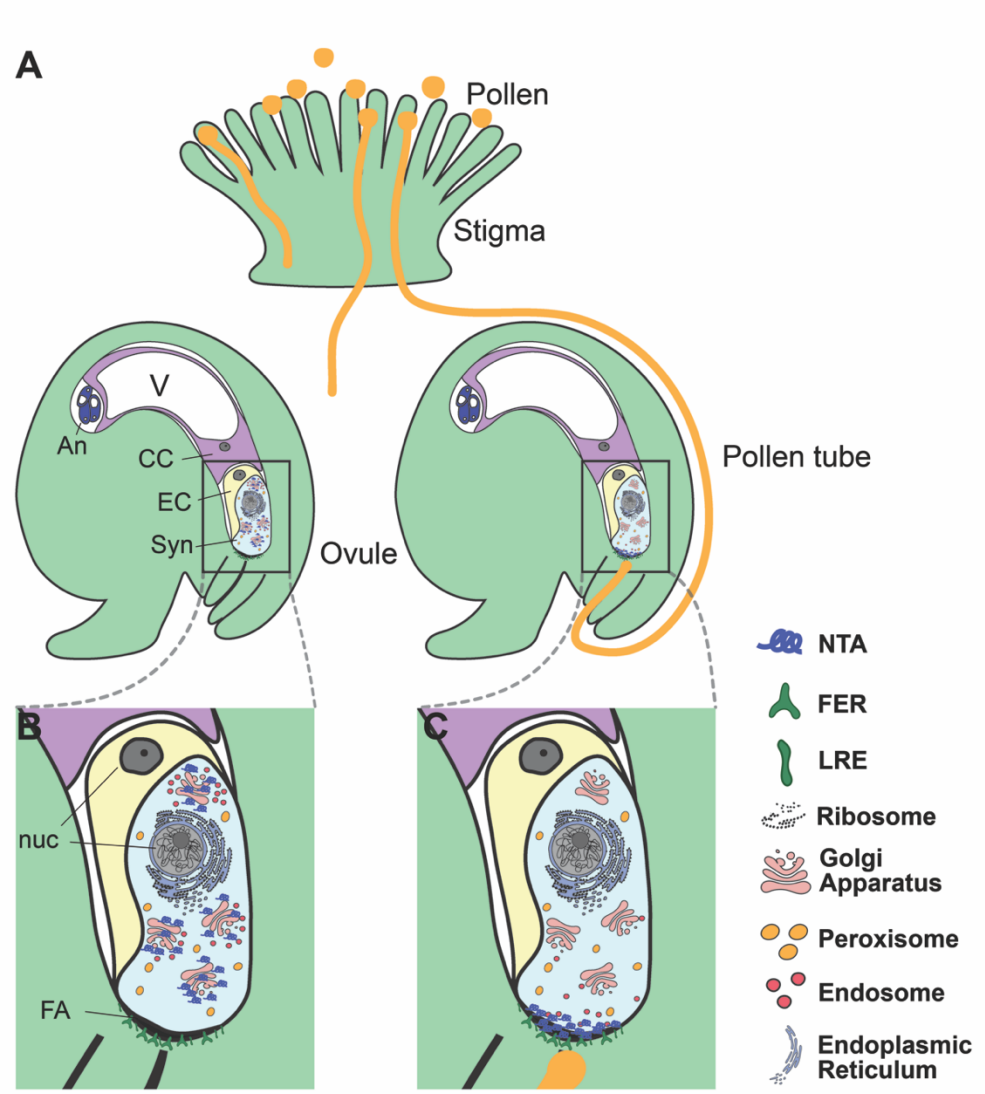

Figure 7. Subcellular dynamics in synergids during pollen tube reception. (A) Pollination using a semi-*in vivo* pollen tube guidance assay. (B) Before pollen tube arrival, NTA is in a Golgi-associated compartment and RabA1g endosomes are distributed throughout the synergids. (C) As a pollen tube arrives, NTA and RabA1g endosomes move toward the filiform apparatus (FA). NTA accumulation is dependent on signaling from the FER receptor like kinase, which acts in a complex with LRE. Abbreviations: CC, Central Cell; Syn, Synergid cells; EC, Egg Cell; An, Antipodal cells; nuc, Nucleus; FA, Filiform Apparatus.

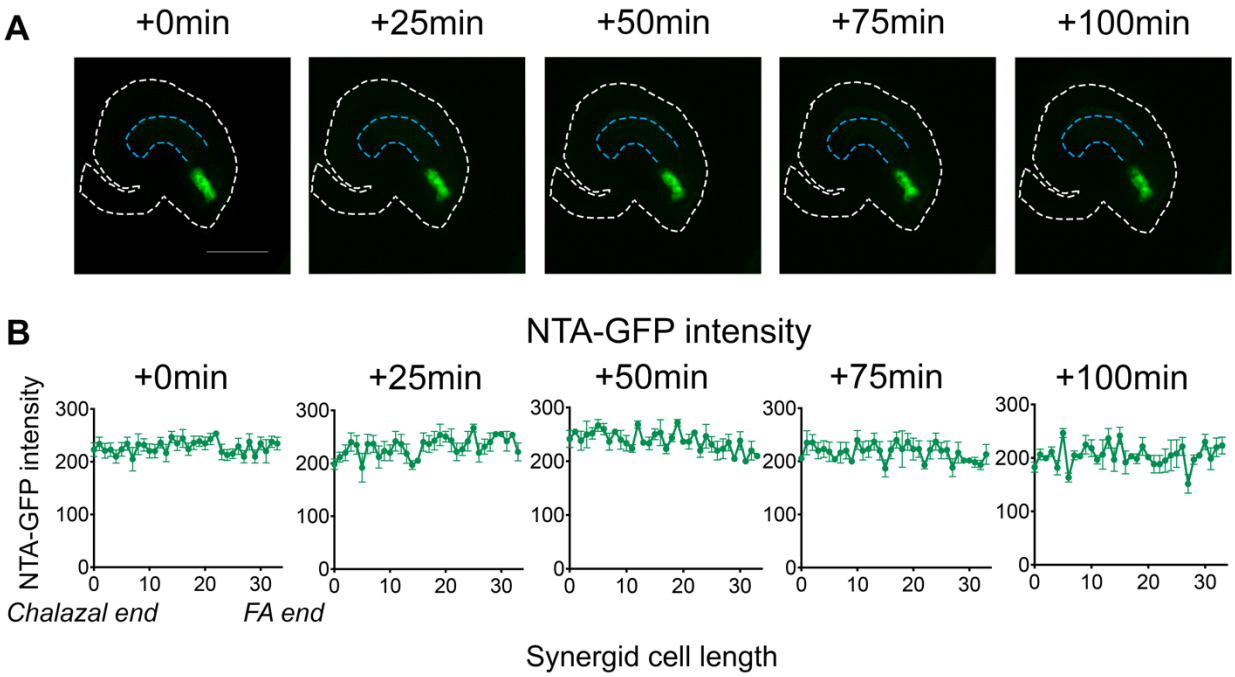

Supplementary figure 1. NTA-GFP does not polarly accumulate at the filiform apparatus in synergids without pollen tube attraction. (A) NTA-GFP (green signal) distribution pattern in synergids at 0min, 25min, 50min, 75min, and 100min timepoints, respectively. (B)Signal intensity measurement of NTA-GFP intensity at 0min, 25min, 50min, 75min, and 100min timepoints, respectively. Bar=50μm.

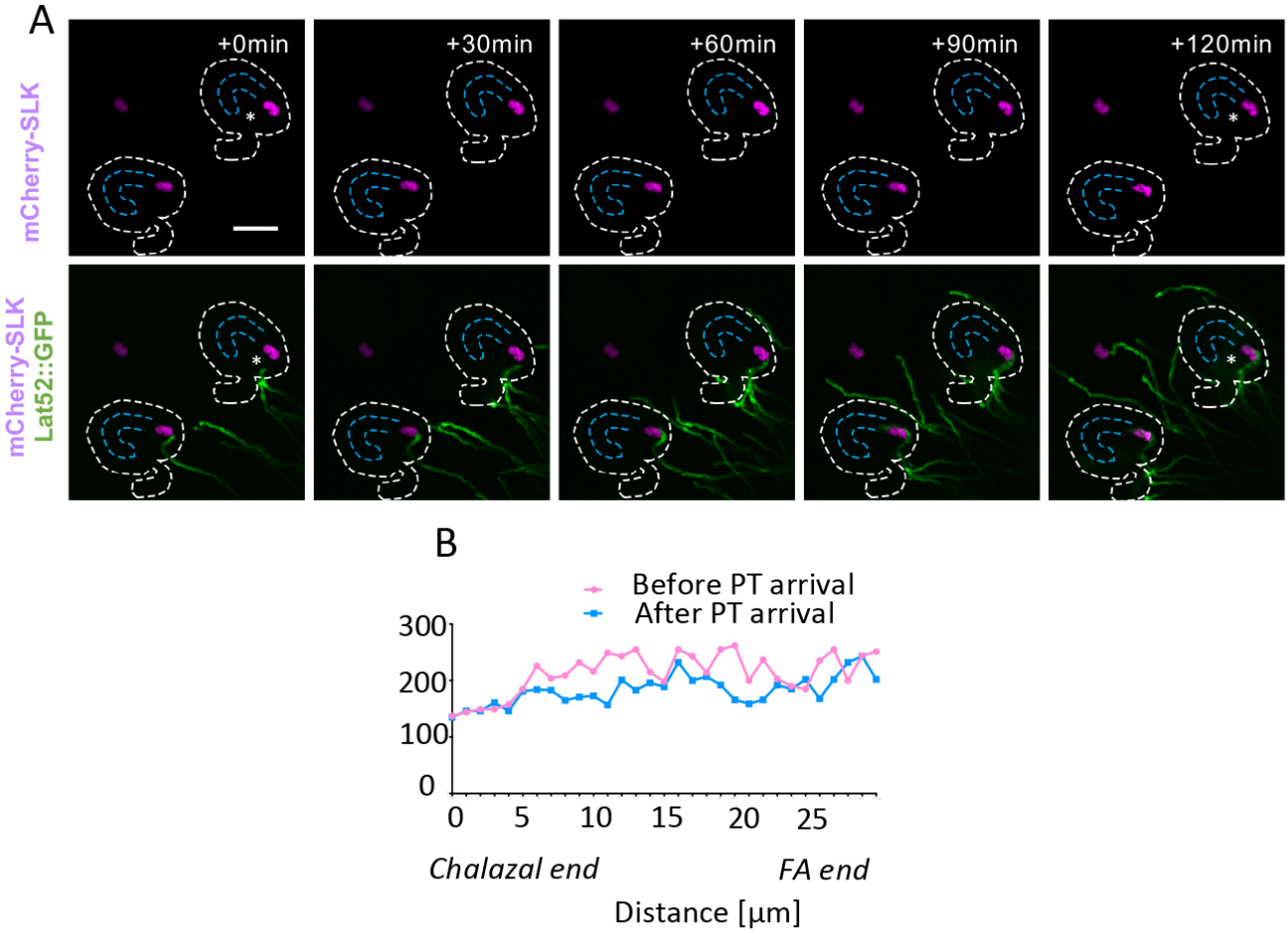

Supplementary figure 2. Peroxisomes do not exhibit polar accumulation at the FA during pollen tube reception. (A) The peroxisome marker mCherry-SLK (magenta signal) does not accumulate to the FA region after pollen tube (green signal) arrival (ovules with green stars). (B) Quantification of mCherry-SLK signal before and after PT arrival. Bars=50µm.

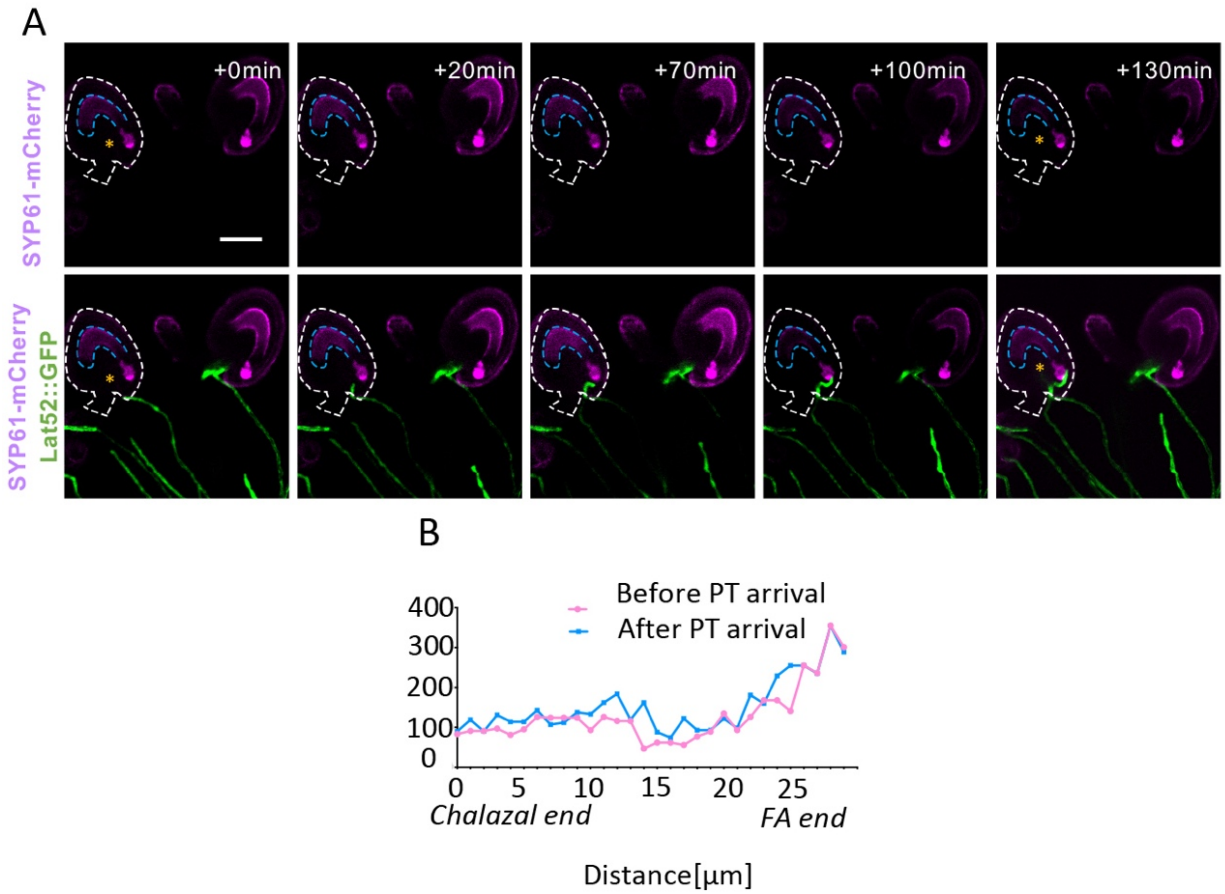

Supplementary figure 3. Trans-Golgi marker distribution in synergids does not change in response to pollen tube reception. (A) The trans-Golgi marker SYP61-mCherry (magenta signal) is concentrated toward the micropyle region of synergid cells both before and after pollen tube (green signal) arrival (ovules with yellow stars). (B) Quantification of SYP61-mCherry signal along the length of a synergid before and after pollen tube reception. Bars=50µm.

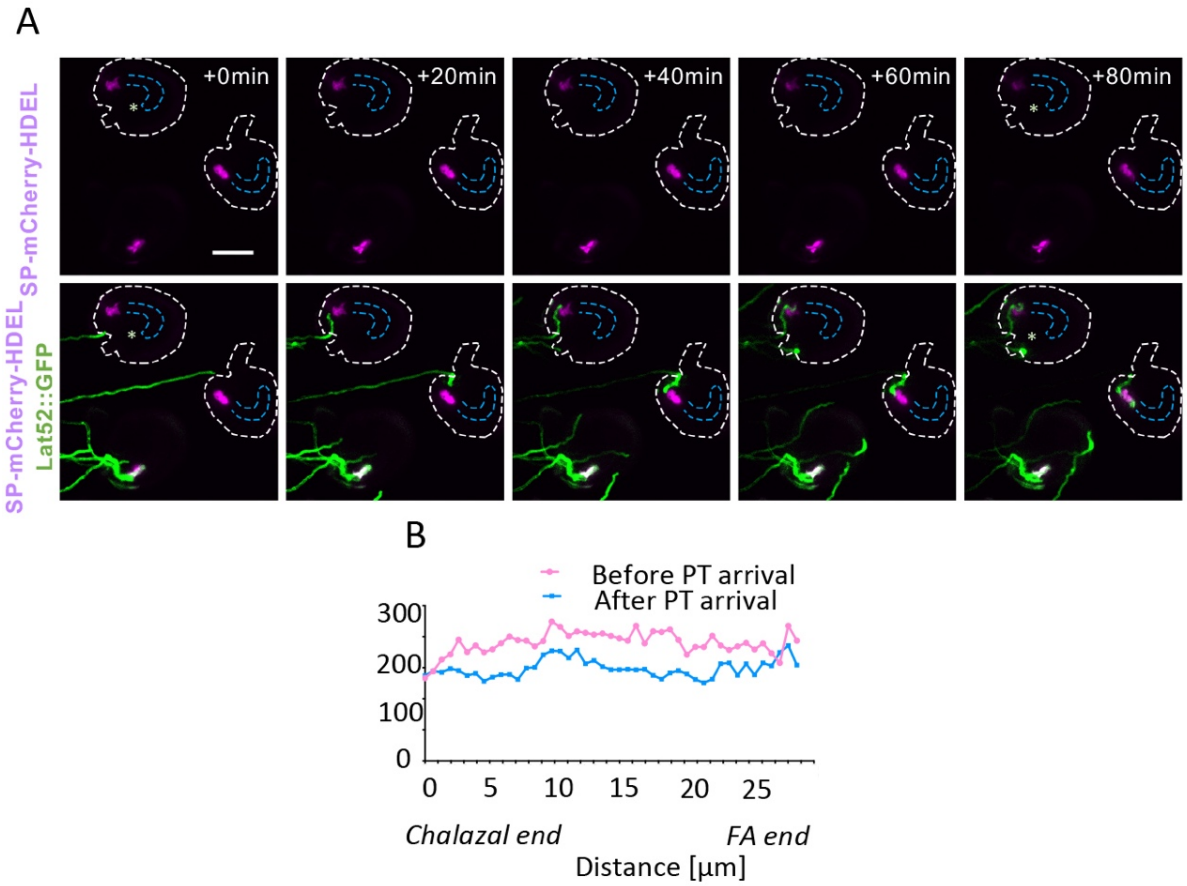

Supplementary figure 4. ER marker distribution in synergids does not change in response to pollen tube reception. (A) Before and after pollen tube (green signal) arrival, the ER marker SP-mCherry-HDEL (magenta signal) is distributed throughout synergid cells (ovules with white stars). (B) Quantification of SP-mCherry-HDEL signal along the length of synergids before and after pollen tube reception. Bars=50µm.

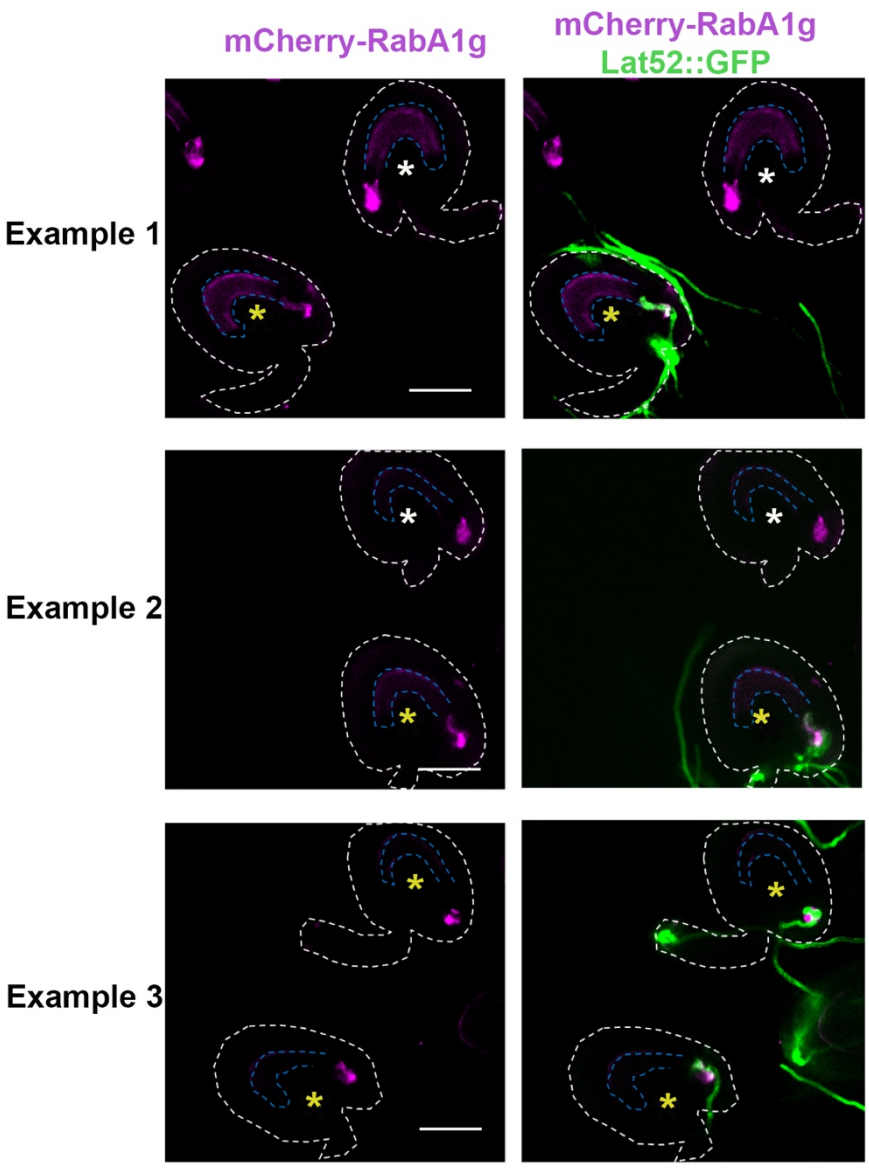

Supplementary figure 5. **Additional examples of the polar accumulation of RabA1g endosomes during pollen tube reception.** Endosome marker accumulates near the filiform apparatus region as pollen tube approaches (ovules with white stars), but no polar accumulation was found in ovules that did not attract a pollen tube (ovules with yellow stars). Bars=50μm.

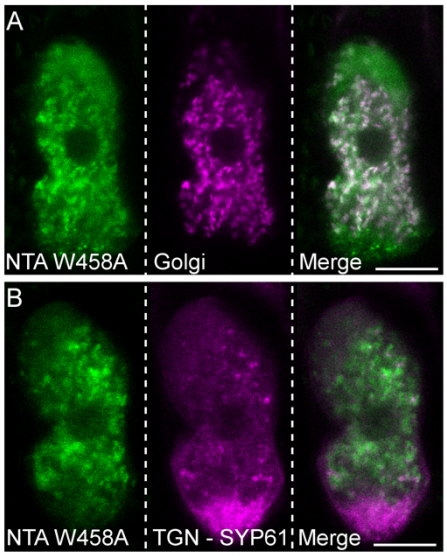

Supplementary figure 6. NTA^{W458A} co-localizes with Golgi marker in synergid cells before pollen tube arrival. Colocalization of NTA^{W458A}-GFP (green) with Golgi marker (LRE:proMan49-mCherry, magenta) (A) and the trans-Golgi network marker (TGN, MYB98pro:SYP61:mCherry, magenta) (B) in the synergid cell of unpollinated ovules. Bars = 10 μm.

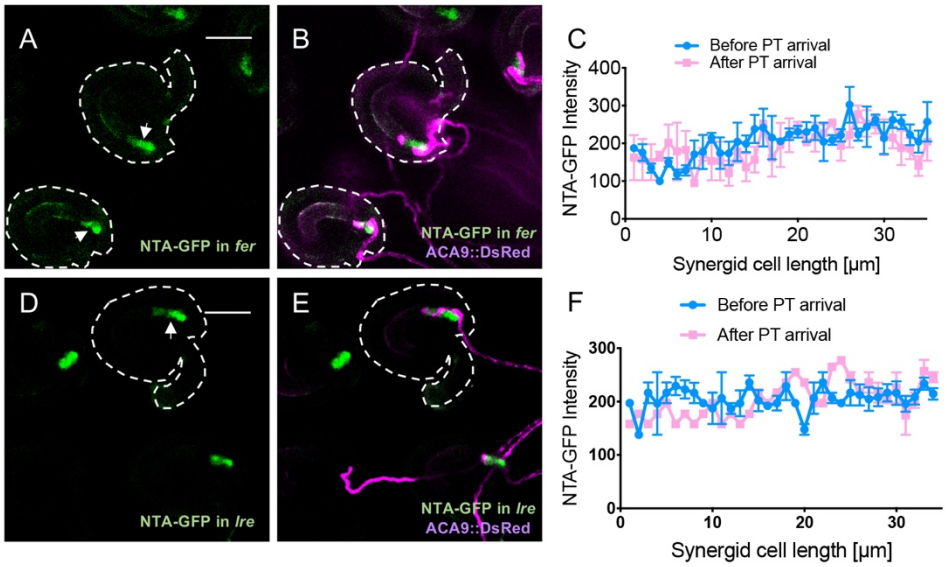

Supplementary figure 7. **NTA-GFP polar accumulation requires FER and LRE.** (A-B) In *fer* mutant synergids, NTA-GFP (green signal) distributes throughout synergids (arrows) with ACA9::DsRed pollen tube overgrowth (magenta signal). (C) Quantification of NTA-GFP signal along the length of *fer-1* synergids before and after pollen tube reception. (D-E) In *lre-7* ovules, NTA-GFP distributes throughout synergids (white arrow) with pollen tube overgrowth. (F) Quantification of NTA-GFP signal along the length of *lre-7* synergids before and after pollen tube reception. FA, Filiform Apparatus. Bars=50μm.

Supplementary table 1. List of primers used for cloning.

Primer Name	Primer Sequences (5' to 3')
NTA481-RattB2	GGGGACCACTTTGTACAAGAAAGCTGGGTGTGAAACACCAAGTGTCTTGCT
NTAW458A-F	GCATTGAAGAAG**GC**GCACAAAGACATCAAATTGAAGAAAG
NTA-RattB2	GGGGACCACTTTGTACAAGAAAGCTGGGTGAGAGTTGTGGAATTGCATCTC
NTA-FattB1	GGGGACAAGTTTGTACAAAAAAGCAGGCTTCACCATGATCACAAGAAGCAGGTGT
NTAW458A-R	C**GC**CTTCTTCAATGCCTTTGCCAT
NTA-R19	CTCATCAAACACTGCTTTCTTCATG
MLO1-F	GCAGTGTTTGATGAGAATGTGCAGGTTGGTCTTGTTG
MLO1-RattB2	GGGGACCACTTTGTACAAGAAAGCTGGGTGGTTGTTATGATCAGGTGTAATCTCA